Development of Kinetic Parameterization Methods for Nitrifying Bacteria using Respirometry

Kyle Malin

Thesis submitted to the faculty of the Virginia Polytechnic Institute and State University in partial fulfillment of the requirements for the degree of

Master of Science
In
Environmental Engineering

Zhiwu Wang
Charles B. Bott
Amy Pruden

10/22/2021

Keywords: Ammonia oxidizing bacteria (AOB), nitrite oxidizing bacteria (NOB), oxygen uptake rate (OUR), oxygen half-saturation (K_O)

Development of Kinetic Parameterization Methods for Nitrifying Bacteria using Respirometry

Kyle Malin

ABSTRACT

Understanding how nitrifiers react when exposed to low DO conditions could provide a greater understanding of low DO operations in full-scale biological wastewater treatment. Previous methods to observe nitrifier oxygen kinetics do exist in literature, however they are inefficient and labor intensive. Other more efficient methods require the use of selective inhibitors, which alter the characteristics of the biomass. This study developed a time and labor efficient respirometric method to distinctly measure oxygen half-saturation coefficients for both ammonia oxidizing bacteria (AOB) and nitrite oxidizing bacteria (NOB) without the use of selective inhibitors. By eliminating the use of inhibitory substances, representative biomass characteristics were maintained throughout the tests. The developed method, called the declining DO method, consisted of using a high-speed dissolved oxygen (DO) probe to measure relative oxygen uptake rates (OUR) within a batch reactor when varying substrates (ammonia and nitrite) were present in excess within the system. A forward model was developed based on Monod kinetics to simultaneously fit Monod curves to the experimental OUR data. These curves were fit by solving for optimum oxygen kinetic parameters representing endogenous respiration, NOB, and AOB. An inverse model using Markov chain Monte Carlo analysis was applied to the results found in the forward model to provide statistical validation of the proposed respirometric method. A separate method, called the substrate utilization rate test, was conducted in parallel with the declining DO tests to compare and verify oxygen half-saturation coefficient results. Parallel tests were conducted using biomass samples from three different Hampton Roads Sanitation District (HRSD) full-scale facilities. Operating conditions between the three HRSD facilities were considered when performing parallel testing, including averages for DO, solids retention time (SRT), and floc size. Average floc size was found to have a significant effect on the observed oxygen half-saturation values. Observed trends for the K_O values estimated using the two methods remained consistent throughout all tests, where $K_{O,NOB}$ was always lower than $K_{O,AOB}$. The comparison of the two methods highlighted some faults associated with the substrate utilization rate test, which is commonly used in literature to observe nitrifier oxygen kinetics. The declining DO method appeared to be more resistant to potential experimental error and required less than half the time compared to the substrate utilization rate test. The development of the declining DO method without the use of selective inhibitors provided a more time and labor efficient technique for estimating apparent K_O values for NOB and AOB without sacrificing biomass characteristics representative of the full-scale treatment process. Biomass samples collected from variable treatment process conditions yielded consistent parallel test results, providing further evidence that the proposed declining DO method can be a robust and reliable technique for distinctly measuring apparent oxygen half-saturation values for NOB and AOB.

Development of Kinetic Parameterization Methods for Nitrifying Bacteria using Respirometry

Kyle Malin

GENERAL AUDIENCE ABSTRACT

Wastewater treatment operations utilizing biological nitrogen removal (BNR) require a continuous supply of oxygen for aerobic processes. Energy costs associated with aeration generally accounts for at least 50% of the total energy consumption at conventional activated sludge wastewater treatment facilities. Operating aerobic zones at low average dissolved oxygen (DO) concentrations could be an effective way to significantly reduce aeration costs as well as material costs associated with BNR treatment processes.

This study developed a method to measure oxygen kinetics for the two groups of autotrophic bacteria responsible for performing nitrogen removal. The method consisted of measuring relative oxygen uptake rates (OUR) within a batch reactor when varying substrates were available. This method is unique from previously developed techniques in that the use of selective inhibitors was not included, meaning the characteristics of the wastewater were largely unchanged and therefore better represent biomass conditions within the full-scale process. The results of the proposed method were verified using an alternate method for estimating oxygen kinetics. These two methods were conducted in parallel using biomass samples from several full-scale Hampton Roads Sanitation District wastewater treatment facilities utilizing a variety of process designs and operating conditions. Consistent results obtained between the two methods suggested the proposed method is an effective technique for distinctly measuring nitrifier oxygen kinetics.

Acknowledgements

I would like to thank Dr. Charles Bott for the incredible opportunity of being a part of his research group. I have truly grown as a person in my time here as a graduate student and research intern and am so appreciative of the experience and everything I have gained. I would also like to thank my research committee members, Dr. Drew Wang and Dr. Amy Pruden, for the time and guidance they've given me as I progressed through this program.

I would like to thank Kester McCullough for being such a great friend and mentor throughout my time in the program. I've learned a great deal from you, and all the guidance you've provided me over the last two years has been invaluable.

To all my fellow research interns, Anand Patel, Kayla Bauhs, Sam Hogard, Tyler Kisling, Hannah Stohr, Mack Pierce, and everyone else working with HRSD: it has been an absolute pleasure becoming friends with you all over the last two years. My graduate experience was made all the better thanks to you.

Thank you to Hampton Roads Sanitation District for providing the funding for my education and aiding in my research. HRSD is truly a great place to work, and that's thanks to all the wonderful people I've had the pleasure of working with and learning from over the last two years.

Finally, I'd like to thank all my friends and family back home in Wisconsin for their unending love and support. I will forever appreciate the confidence you instill in me to take risks in pursuit of my goals.

Table of Contents

List of Tables

List of Figures

1. Introduction

Wastewater treatment is an expensive yet necessary process to protect public health and natural resources. As restrictions on effluent limits in the United States become more stringent, the process only becomes more costly. Energy costs make up a significant portion of the expenses associated with wastewater treatment. In 2011, municipal wastewater treatment processes in the Unites States alone accounted for 0.8% of the country's total electricity consumption (Liu & Wang, 2015). As the country's population continues to rise, this will only increase demand on wastewater treatment infrastructure in the future. These reasons provide ample motivation for research into the advancement of wastewater treatment to make these processes more cost effective and energy efficient. Wastewater treatment plants (WWTPs) that utilize biological treatment require a continuous supply of oxygen for aerobic biological processes, particularly nitrification. It is known that aeration costs generally account for at least 50% of a WWTP's total energy consumption (Bertanza et al. 2021).

One promising strategy for reducing costs associated with biological nutrient removal is by operating aerobic zones at lower dissolved oxygen (DO) concentrations. WWTPs typically provide more than enough DO for full nitrification. The potential benefits to low DO operation are not limited to a reduction in aeration energy requirements. Lower concentrations of DO within the aerobic zone result in less DO recycled back to the first anoxic zone as well as less DO sent to the second anoxic zone, preserving carbon present within the influent wastewater for denitrification purposes. If influent carbon is available, simultaneous nitrification-denitrification (SND) is possible in the aerobic zone, which could ultimately lead to a reduction in costs associated with external carbon addition. SND can also lead to a reduction in costs due to alkalinity addition, as alkalinity produced through denitrification can in turn be used for nitrification. Combining a low DO process with the implementation of advanced aeration controls like ammonia-based aeration control (ABAC) or ammonia vs. NO_X (AvN) can result in a desired residual ammonia concentration after the aerobic zones. The retained ammonia concentration implies less oxygen demand and could also be utilized in advanced treatment processes like partial denitrification annamox (PdNA). Residual ammonia concentration after the aerobic zone can also lead to a decrease in hypochlorite addition for disinfection purposes through monochloramine production.

One of the immediate issues associated with operating aerobic zones at low DO concentrations is the reduction in nitrification rates, requiring a longer aerobic SRT to achieve the desired level of ammonia removal. Reduced nitrification rates result in an overall reduction in treatment capacity for a WWTP, which is not feasible for plants already operating towards their upper capacity limits. However, recent studies have found evidence that aerobic zones can be operated at low DO concentrations without a significant reduction in nitrification capacity after an acclimation period (Fan et al., 2016; Keene et al., 2017; Wen et al., 2020). This could signify nitrifier physiological adaptation, or a shift toward nitrifier communities better suited to

perform nitrification in low DO conditions. It is hypothesized that ammonia oxidizing bacteria (AOB) and nitrite oxidizing bacteria (NOB) can regain nitrification capacity when exposed to low DO conditions for an extended period of time.

The Monod equation is frequently used in wastewater treatment to model biological rates, most commonly representing exponential growth as a function of substrate concentration within the system. The research presented by Shaw (2015) demonstrated that the substrate half-saturation coefficient (K_S), a value critical for describing biological processes within wastewater treatment, is not a constant but rather a function of the maximum rate exhibited by that biological group. Accounting for the variability of K_S provided more accurate substrate removal models, which could ultimately lead to more informed design considerations for full-scale treatment processes. If nitrifiers do have the potential to adapt to low DO conditions, the expectation is that their respective oxygen half-saturation values will decrease (or increase their affinity for oxygen) when exposed to decreased DO concentrations over time. Besides the more common use for estimating microbial growth rates in wastewater systems, the Monod equation can be used to estimate nitrifier oxygen kinetics when extended to oxygen uptake rate (OUR). In this form, oxygen is the measured substrate being consumed. The Monod equation in terms of OUR is shown in equation 1 below:

$$OUR = OUR_{max} * \frac{DO}{K_o + DO} \quad (1)$$

Where:

OUR	= Oxygen uptake rate (mg O_2/L/hr)
OUR_{max}	= Maximum oxygen uptake rate (mg O_2/L/hr)
S_O	= Dissolved oxygen concentration at any point in time (mg O_2/L)
K_o	= Oxygen half-saturation coefficient (mg O_2/L)

K_O is defined as the oxygen concentration at which the observed OUR is half of the maximum OUR value. A curve can be created using the Monod equation to estimate oxygen kinetic parameters. Figure 1 shows a set of Monod curves and the key oxygen kinetic parameters involved, highlighting how a change in K_O will affect the resulting curve.

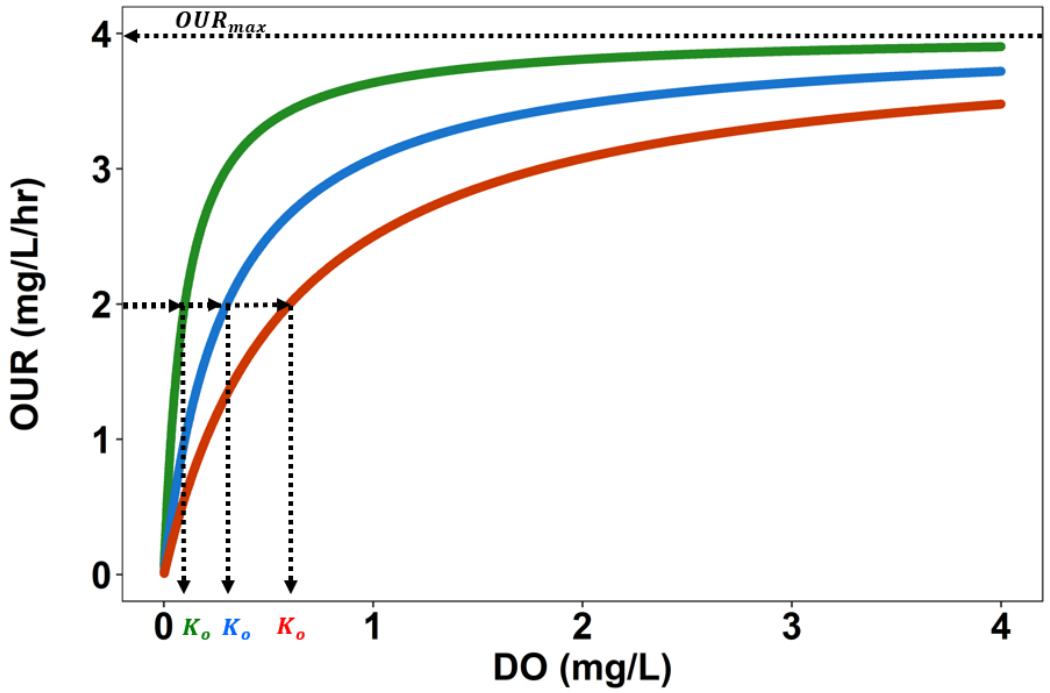

Figure 1. Monod curves in terms of oxygen uptake rate (OUR), with maximum oxygen uptake rate (OUR_{MAX}) and respective oxygen half-saturation (K_O) values identified for each curve.

The curves shown in Figure 1 were created using the Monod equation in terms of OUR (equation 1). Each curve has an OUR_{max} value of 4 mg O_2/L and different values for K_O. This graph highlights the significance of the K_O value in terms of OUR as DO concentration changes. As DO concentrations decrease, a functional group with a lower observed K_O value is capable of consuming oxygen at a rate closer to the observed maximum OUR. In terms of competition, if each of these curves represented a different functional group of respiring bacteria, the group represented by the green curve would be more advantaged in lower DO conditions compared to the groups represented by the blue and red curves.

To observe potential nitrifier adaptation to low DO conditions, a method to distinctly measure the oxygen half saturation for both AOB and NOB must be utilized. Two main methods exist in literature to measure oxygen-half saturation values for nitrifiers. The first, called the declining DO method, is a relatively simple experiment that measures the DO drop, or relative oxygen uptake rate (OUR), within a mixed reactor when various substrates are present in excess. The relative OUR curves are fit using the Monod equation and used to estimate relative oxygen kinetic parameters for nitrifiers. In the work presented by Guisasola et al. (2005), the declining DO method was utilized to distinctly measure K_O for both NOB and AOB ($K_{O,NOB}$ and $K_{O,AOB}$, respectively). To observe AOB independently of NOB when ammonia is present in the system, selective inhibitors (sodium azide) are also introduced to inhibit NOB acting on nitrite produced through nitritation. Other works that employ a similar method include Ghimire (2012) and De Mulder (2014), all utilizing selective inhibitors in a similar way. The issue with selective inhibitors is that the characteristics of the biomass are changed and therefore no longer fully represent the conditions found within a full-scale treatment facility.

The second method commonly utilized in literature to estimate oxygen half-saturation coefficients for nitrifiers is referred to as the substrate utilization rate method. This test procedure consists of establishing various DO concentration setpoints within a mixed reactor and measuring the relative substrate removal/production rates (R) at each setpoint. A curve can be fit to the relative substrate utilization rates determined at each DO concentration using a Monod equation of the form:

$$R = R_{max} * \frac{S_O}{K_O + S_O} \quad (2)$$

The resulting curve fits can be used to estimate oxygen half-saturation values for NOB and AOB. An early example of this method can be found in Sanchez et al. (2001) and was applied in later works such as Ghimire (2012), De Mulder (2014) and Keene et al. (2017). While this method does not require the use of selective inhibitors to estimate nitrifier oxygen kinetics like the declining DO method, it does require a significant amount of time (upwards of 8 hours) and labor to execute properly. In addition to the extensive time and labor requirements, the test only yields a handful of nitrifier rate values to which a Monod curve can be fit. Any error associated with one or more of those rate estimations can significantly affect the estimated oxygen kinetics.

The objectives of this work were to develop a time and labor efficient method to distinctly measure the oxygen half-saturation coefficients for NOB and AOB within an activated sludge reactor. Maintaining representative biomass characteristics was a priority, therefore the use of selective inhibitors was avoided. Nitrifier oxygen half-saturation coefficients found using the developed method were validated by conducting a different kinetic testing method in parallel under identical experimental conditions. By comparing the results obtained using the two methods, it was possible to judge the legitimacy of the developed testing method. These parallel tests were applied to multiple full-scale WWTP biomasses utilizing various operating conditions, including two BNR activated sludge treatment facilities and one membrane bioreactor (MBR) treatment facility.

2. Literature Review

Biological Nitrogen Removal

Biological Nitrogen Removal is an essential process used in biological wastewater treatment facilities around the world. Typical wastewater treatment plant (WWTP) influent flow contains nitrogen species primarily consisting of ammonia (NH_3), or the ionized form ammonium (NH_4^+). The presence of ammonia in aquatic environments has a long list of detrimental effects which includes changes in species growth, decrease in species diversity, and fish kills. High concentrations of ammonia increase the biological oxygen demand in that system, where then microbes will grow and consume oxygen beyond a point at which fish can survive. Excess concentrations of nitrogen can also provide fuel for plant growth, leading to a proliferation of algae (algal blooms) called eutrophication (EPA, 2021). Algal blooms can inhibit sunlight penetration for aquatic vegetation and decaying plant biomass leads to critically low dissolved oxygen concentrations than required to sustain aquatic species. For those reasons, government regulatory agencies impose upper limits for contaminants like inorganic nitrogen for wastewater treatment effluent streams discharged to the environment. Contaminant concentrations are used as key indicator of treatment performance throughout the process.

This work focuses on the first half the biological nitrogen removal process known as nitrification, which is an aerobic process carried out by autotrophic bacteria in two steps: *nitritation* and *nitratation*. Nitritation is performed by ammonia oxidizing bacteria (AOB), where ammonia is converted into nitrite. Nitratation is performed by nitrite oxidizing bacteria (NOB), where nitrite is converted into nitrate. In both cases, oxygen is used as an electron acceptor and is therefore necessary for these processes to occur (Jubany et al., 2005). Stoichiometries for nitritation and nitratation reactions are shown in equations 3 and 4, respectively.

$$NH_4^+ + \frac{3}{2}O_2 \rightarrow NO_2^- + 2H^+ + H_2O \quad (3)$$

$$NO_2^- + \frac{1}{2}O_2 \rightarrow NO_3^- \quad (4)$$

Monod Kinetics

The fundamental basis of the method proposed within this work utilizes Monod Kinetics. The Monod equation (5) has been used since the early 1940s to describe the exponential growth of bacteria based on substrate concentrations (Grady et al., 2011).

$$\mu = \hat{\mu}\frac{S}{K_S+S} \quad (5)$$

Where:

μ = Specific growth rate at any substrate concentration

$\hat{\mu}$ = Maximum specific growth rate
S = Substrate concentration at any point in time
K_S = Substrate half-saturation coefficient

The value K_S determines how quickly the specific growth rate approaches the maximum specific growth rate depending on the substrate concentration within the system. K_S defines the substrate concentration at which the specific growth rate is half of the maximum specific growth rate. While most often used to estimate the specific growth rate for a bacteria group within the field of biological wastewater treatment, the Monod equation can also be extended to oxygen uptake rate (OUR):

$$OUR = OUR_{max} \frac{S_O}{K_o + S_O} \quad (6)$$

Where:

OUR = Oxygen uptake rate
OUR_{max} = Maximum oxygen uptake rate
S_O = Dissolved oxygen concentration at any point in time
K_o = Oxygen half-saturation coefficient

Using the Monod equation in this form treats oxygen as the substrate and provides the ability to estimate OUR at any point in time as a function of the DO concentration present within the system. Like K_S, the oxygen half-saturation (K_O) value represents the DO concentration at which the observed OUR is half of the maximum OUR. In an oxygen-rich environment, aerobic bacteria consume oxygen at a rate close to their maximum rate. As the oxygen concentration within the system decreases, oxygen consumption for aerobic bacteria is reduced. The K_O value dictates how great of an affect a decreasing oxygen concentration will have on aerobic bacteria respiration. Using the Monod equation in terms of OUR provides the ability to use respirometry to measure nitrifier oxygen kinetics and observe how changing DO concentrations affect nitrification rates.

Respirometry

Microbial respiration is the metabolic process in which adenosine triphosphate (ATP) is generated through electron transfer. ATP provides energy for cells to carry out operations like growth, maintenance, and reproduction (van Loosdrecht et al., 2016). Electron donors, like ammonia and nitrite, are converted to their oxidized form (nitrite and nitrate, respectively) where oxygen serves as the terminal electron acceptor. Respirometry has been used to measure biological oxygen consumption rates since the early 1900s, but since the 1980s it has become an important tool with the development of activated sludge modelling (Ordaz et al., 2008; Torretta et al., 2014). With technological advancements in instrumentation, more accurate kinetic information can be gained using various respirometry techniques. Respirometry can be used to estimate values for the substrate half-saturation (K_S), substrate oxidation yield (f_E), the maximum substrate degradation rate (R_{max}), the maximum growth

rate ($\hat{\mu}$), oxygen half-saturation (K_O), and the biomass growth yield (f_E) (Chandran & Smets, 2005; Guisasola et al., 2005; Pai et al., 2010). Respirometry can provide a great deal of valuable information about activated sludge biomass characteristics which can be used to increase the accuracy for activated sludge models. The methods discussed within this work were primarily focused on distinctly measuring K_O for both NOB and AOB.

Intrinsic vs. Extant kinetics

When considering techniques for measuring oxygen kinetics in BNR processes, a distinction must be made between intrinsic and extant values. An intrinsic value in wastewater kinetics describes the physiological state of an organism and its ability to carry out its biological functions. A measurement for the intrinsic K_O value represents the oxygen half-saturation exhibited by a single cell within a system without any limitations associated with the wastewater characteristics or process operating conditions. Extant (or apparent) K_O represents the oxygen half-saturation observed within the existing wastewater conditions which incorporates all potential limitations associated with that (Val del Rio et al., 2019). In terms of real-world applications, apparent kinetic measurements are valuable for wastewater treatment design as those are the values exhibited within the process. The methods outlined within this work ultimately measure the apparent value for nitrifier oxygen half-saturation, which will be implied hence forth unless otherwise stated.

Floc Morphology

The need to distinguish between intrinsic and apparent values in terms of oxygen kinetics is largely due to floc morphology. The relative size and density of flocs can vary greatly between WWTPs depending on a variety of factors including operating conditions and influent wastewater characteristics. Larger, more dense flocs experience greater declines in DO concentrations with respect to floc depth (Daigger et al., 2007). This phenomenon results in an overall reduction in oxygen exposure for microorganisms closer to the center of the floc relative to the bulk solution. Figure 2 depicts a theoretical representation of relative dissolved oxygen concentrations as a function of depth within a spherical floc.

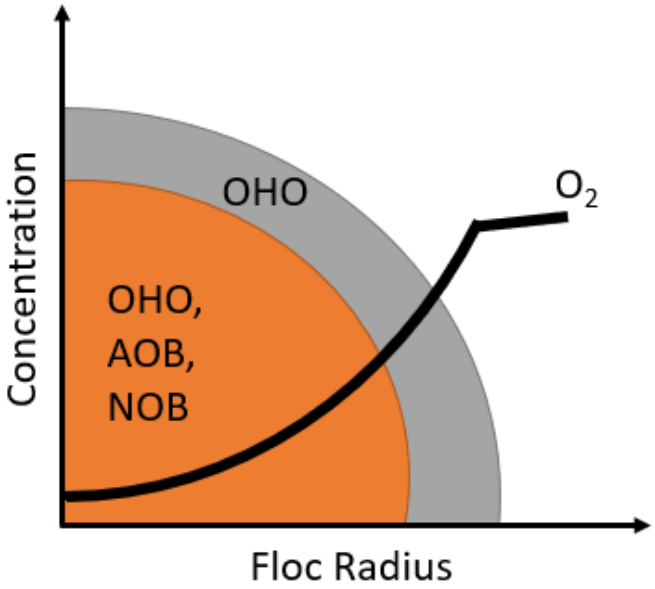

Figure 2. Theoretical slice of activated sludge floc where the outer layer is predominantly made up of ordinary heterotrophic organisms (OHO) and the inner layer consisting of a combination of OHO, AOB and NOB (figure adapted from Manser et al. (2005)).

Small flocs, such as those found in membrane bioreactors (MBRs), experience less oxygen mass transfer limitation, and therefore exhibit K_O values more representative of intrinsic values (Manser et al., 2005). Conventional activated sludge (CAS) processes generally form larger flocs and therefore experience greater mass transfer limitations, resulting in higher observed values of K_O (Picioreanu et al., 2016). As the DO concentration within the bulk solution decreases, nitrifiers clustered within larger flocs will experience a scarcity of oxygen sooner (at higher DO concentration) compared to nitrifiers in smaller flocs. Due to the relationship with floc morphology, apparent oxygen half-saturation values are sludge dependent and therefore should be treated as such between different treatment plants and processes (De Mulder, 2014). A short summary for various studies that measured K_O values in wastewater from CAS (Table 1) and MBR (Table 2) sources can be found below.

Table 1. Literature K_O values for NOB and AOB measured using biomass sourced from CAS WWTPs.

$K_{O,NOB}$ (mg O_2/L)	$K_{O,AOB}$ (mg O_2/L)	Source
0.47 ± 0.04	0.79 ± 0.08	Manser et al. 2005
0.23 ± 0.09	0.65 ± 0.07	Daebel et al. 2006

Table 2. Literature K_O values for NOB and AOB measured using biomass sourced from MBR WWTPs.

$K_{O,NOB}$ (mg O_2/L)	$K_{O,AOB}$ (mg O_2/L)	Source
0.13 ± 0.06	0.18 ± 0.04	Manser et al. 2005
0.28 ± 0.03	0.42 ± 0.09	Daebel et al. 2006

Microbial Adaptation

Activated sludge models commonly use the Monod function to estimate biological growth and performance in wastewater processes, and often treat the half-saturation coefficient (K_S) as a constant. The research performed by Shaw (2015) demonstrated that K_S is not a constant but rather a function of the maximum rate exhibited by that biological group. When considering this value to be constant in varying conditions, this could lead to an underestimation, or overestimation, in biological process performance. Shaw (2015) highlighted situations in which considering the variability of K_S to be critical, one of which is when desired effluent concentrations for substrate are low. In the case of nitrification, target effluent ammonia concentrations are very low compared to that of the influent wastewater. When ammonia concentrations are high, the chosen Ks value has little effect on the resulting oxidation rates. However, as ammonia concentrations are reduced through nitritation, the value of K_S becomes more important and ultimately has a greater effect on the observed oxidation rates for ammonia. In the case of operating aerobic zones at low DO concentrations, using the Monod function to estimate oxygen kinetics means the consideration of K_O as a variable is critical to understanding nitrifier performance within those conditions.

When exposed to low DO conditions (<0.2 mg O_2/L) for long periods, nitrifiers have demonstrated the ability to recover almost all the nitrification capacity lost from the initial reduction in DO (Keene et al., 2017). A variety of studies have observed a decrease in apparent nitrifier K_O values when exposed to low DO conditions for extended periods of time, suggesting a microbial response to the operating conditions (Fan et al., 2016; Keene et al., 2017; & Wen et al., 2020). This shift in observed nitrifier oxygen kinetics could be physiological response to the changing DO conditions. Any observed physical change in floc morphology based on variable DO conditions could also lead to a change in observed K_O due to varying oxygen mass transfer limitations. Changes to nitrifier communities whether physiological, physical, or a combination of both, could explain the observed nitrifier adaptation. Additional research is required to better understand how nitrifier communities respond to low DO conditions.

Measurement methods that have been developed and tested

As previously stated, respirometry can be used to measure a long list of kinetic parameters for activated sludge biomass, and this work was primarily focused on measuring oxygen half-saturation for NOB and AOB. Various methods for measuring nitrifier K_O values already exist in modern wastewater treatment research; however, these methods do have limitations. Two specific methods used to estimate K_O values for nitrifiers established within literature will be highlighted. Within this work, these methods will be referred to as the “declining DO” method and the “substrate utilization rate” method. The details of these two methods will be discussed within the following two sections.

Declining DO Method

The declining DO method (a variation of which is the focus of this work) is a relatively simple experiment that measures the DO drop, or relative oxygen uptake rate (OUR), within a reactor when various substrates are present. In the work presented by Guisasola et al. (2005), the declining DO method was utilized to distinctly measure K_O for both NOB and AOB ($K_{O,NOB}$ and $K_{O,AOB}$, respectively). The procedure as described by Guisasola et al. (2005) begins by establishing a steady state DO concentration, where the mass of air supplied to the system is approximately the same as the endogenous respiration rate within the reactor. After a steady state DO concentration is established, non-limiting amounts of substrate (either ammonia or nitrite) is pulsed into the system, which results in an observed increase in OUR. Higher rates of oxygen consumption cause a sudden drop in DO from the previously established steady state DO concentration. When a new steady state DO concentration has been reached (which implies the maximum OUR has been achieved) aeration is stopped and the resulting change in DO over time within the reactor can be described using equation 7:

$$\frac{dS_O}{dt} = k_L a^{SUP} * [S_O^* - S_O(t)] - (OUR_{END} + OUR_{MAX}) * (\frac{S_0}{K_O + S_O}) \quad (7)$$

Where:

$k_L a^{SUP}$	= global oxygen transfer constant through liquid-gas surface
OUR_{END}	= endogenous oxygen uptake rate
OUR_{MAX}	= maximum oxygen uptake rate after substrate addition
S_O^*	= dissolved oxygen saturation concentration
$S_O(t)$	= dissolved oxygen concentration at any point in time
K_o	= oxygen half-saturation coefficient

The tests conducted in Guisasola et al. (2005) used an uncovered reactor, therefore the inclusion of the $k_L a^{SUP} * [S_O^* - S_O(t)]$ term accounts for the driving force of oxygen diffusing into the reactor from the atmosphere. As the DO concentration within the reactor decreases, this term increases, meaning atmospheric oxygen will more easily diffuse into the reactor through the air-liquid interface. When dosing ammonia to observe the AOB rates, ammonia is converted into nitrite through nitritation. Unless selective inhibitors are introduced into the system, NOB would be free to consume oxygen to facilitate nitration which would affect the observed OUR_{MAX}, thus preventing the ability to observe AOB respiration exclusively. To account for this, sodium azide is added to the system to prevent nitratation from occurring when dosing ammonia. By fitting the experimental data to equation 5, $K_{O,NOB}$ and $K_{O,AOB}$ can be explicitly solved. Guisasola et al. (2005) also considered probe response time and found that it had a significant effect on the results for $K_{O,NOB}$ and $K_{O,AOB}$. DO concentration within the reactor was collected at a frequency of 10/minute. The experimental data for DO concentration was corrected using the following equation 8:

$$S_O^{CORR}(t) = \frac{S_O^{MEAS}(t) - \left(1 - (\frac{\Delta t}{\Delta t + \tau})\right) * S_O^{MEAS}(t-1)}{\Delta t / (\Delta t + \tau)} \quad (8)$$

Where:

S_O^{CORR} = corrected DO measurement
S_O^{MEAS} = measured DO concentration
Δt = data collection frequency
τ = probe response time

Probe response time can be determined experimentally by quickly switching the probe between DO saturated water and zero DO water (water bubbled with nitrogen gas) to determine how much time is required for the probe to register 95% of the total change in DO concentration. The authors explored how correcting the measured DO concentration for probe response time could affect resulting observed $K_{O,NOB}$ and $K_{O,AOB}$, emphasizing the importance of this correction for tests with low data collection frequency. It was found that neglecting to account for probe response time and data collection frequency resulted in an underestimation for both $K_{O,NOB}$ and $K_{O,AOB}$ values. A summary of these results can be found in Table 3:

Table 3. Summary of measured oxygen half-saturation values with 95% confidence intervals determined for NOB and AOB from Guisasola et al. (2005)

	$K_{O,NOB}$ (mg O_2/L)	$K_{O,AOB}$ (mg O_2/L)
Uncorrected	0.49 ± 0.02	1.64 ± 0.01
Corrected	0.74 ± 0.02	1.75 ± 0.01

Examples of other literature utilizing this declining DO method to estimate nitrifier oxygen kinetics includes Ghimire (2012) and De Mulder (2014). In most cases where NOB and AOB oxygen kinetics are distinctly measured using this method, selective inhibitors are used to prevent nitratation from occurring when measuring AOB oxygen half-saturation. While the use of selective inhibitors, like sodium azide, does provide the ability to observe AOB respiration without the interference of NOB activity, they also fundamentally change characteristics of the wastewater being tested. Other works employ a similar method for performing the declining DO test without the use of selective inhibitors and instead treat nitrification as a single step process. This simplification assumes that nitritation is the limiting step in the overall nitrification process, meaning any nitrite resulting from the oxidation of ammonia via AOB is instantly oxidized into nitrate via NOB (Ordaz et al., 2008). This eliminates the need to isolate nitrifier activities and instead evaluates a combined oxygen half-saturation value representing full nitrification. The obvious downside to this strategy is the inability to distinctly observe and compare NOB and AOB respiration rates and ultimately their relative apparent K_O values.

Substrate Utilization Rate Method

The other method for estimating nitrifier oxygen kinetics is the substrate utilization rate method. This test procedure consists of establishing various DO concentration setpoints within a mixed reactor and measuring the relative substrate removal/production rates at each setpoint. An early example of this method can be seen in Sanchez et al. (2001) and was applied

in later works such as Ghimire (2012), De Mulder (2014) and Keene et al. (2017). From the test data, ammonia removal rates are estimated by calculating the slope of the series of substrate data points at each DO setpoint. These removal rates can be plotted versus their respective DO setpoints and fit to a Monod equation of the form:

$$R = R_{max} * \frac{S_O}{K_O + S_O} \quad (9)$$

Where:

R	= substrate removal rate (mg N/gVSS/d)
R_{max}	= maximum substrate removal rate (mg N/gVSS/d)
S_O	= Dissolved oxygen concentration at any point in time
K_o	= Oxygen half-saturation coefficient

By fitting the substrate removal rates estimated at each DO setpoint to equation 9, the K_O value for NOB and AOB can be estimated. One of the biggest drawbacks to this method is the amount of time and labor required. To confidently estimate substrate removal rates, at least six different samples must be collected to determine changes in substrate concentrations at each DO setpoint. If these sample collections are at least ten minutes apart, each DO setpoint would take one hour. Conducting this test at seven different DO setpoints would take at least seven hours, and only provide the same number of substrate removal rates to which a Monod curve can be fit. Since the K_O value determined through this procedure is dependent on the Monod fit, any potential experimental error could affect the results significantly.

References

Bertanza, G., Baroni, P., Garzetti, S., & Martinelli, F. (2021). Reducing energy demand by the combined application of Advanced Control Strategies in a full scale WWTP. *Water Science and Technology*, *83*(8), 1813–1823.

Chandran, K., & Smets, B. F. (2005). Optimizing experimental design to estimate ammonia and nitrite oxidation biokinetic parameters from batch respirograms. *Water Research*, *39*(20), 4969–4978.

Daigger, G. T., Adams, C. D., & Steller, H. K. (2007). Diffusion of oxygen through activated SLUDGE FLOCS: Experimental measurement, modeling, and implications for simultaneous nitrification and Denitrification. *Water Environment Research*, *79*(4), 375–387.

Daebel, H., Manser, R., & Gujer, W. (2007). Exploring temporal variations of oxygen saturation constants of nitrifying bacteria. *Water Research*, *41*(5), 1094–1102.

De Mulder, C. *Impact of Intrinsic and Extrinsic Parameters on the Oxygen Kinetic Parameters of Ammonia and Nitrite Oxidizing Bacteria.* Master's Thesis, University of Gent. 2014

Environmental Protection Agency. Ammonia. (2021). *Causal Analysis/Diagnosis Decision Information System (CADDIS v.2)*. https://www.epa.gov/caddis-vol2/ammonia

Fan, H., Qi, L., Liu, G., Zhang, Y., Fan, Q., & Wang, H. (2016). Aeration optimization through operation at low dissolved oxygen concentrations: Evaluation of oxygen mass transfer dynamics in different activated sludge systems. *Journal of Environmental Sciences*, *55*, 224–235.

Ghimire, B.K. (2000). Investigation of oxygen half saturation coefficients for nitrification. [Master's Thesis, Tribhuvan University, Nepal].

Grady Jr, C.L., Daigger, G.T., Love, N.G., Filipe, C.D., Leslie Grady, C., 2011. *Biological Wastewater Treatment*: IWA Publishing.

Guisasola, A., Jubany, I., Baeza, J. A., Carrera, J., & Lafuente, J. (2005). Respirometric estimation of the oxygen affinity constants for biological ammonium and nitrite oxidation. *Journal of Chemical Technology & Biotechnology*, *80*(4), 388–396.

Jubany, I., Baeza, J. A., Carrera, J., & Lafuente, J. (2005). Respirometric calibration and validation of a biological nitrite oxidation model including biomass growth and substrate inhibition. *Water Research*, *39*(18), 4574–4584.

Keene, N. A., Reusser, S. R., Scarborough, M. J., Grooms, A. L., Seib, M., Santo Domingo, J., & Noguera, D. R. (2017). Pilot plant demonstration of stable and efficient high rate biological nutrient removal with low dissolved oxygen conditions. *Water Research*, *121*, 72–85.

Liu, G., & Wang, J. (2012). Probing the stoichiometry of the nitrification process using the respirometric approach. *Water Research*, *46*(18), 5954–5962.

Liu, G., & Wang, J. (2015). Modeling effects of do and SRT on activated sludge decay and production. *Water Research*, *80*, 169–178.

Manser, R., Gujer, W., & Siegrist, H. (2005). Consequences of mass transfer effects on the kinetics of nitrifiers. *Water Research*, *39*(19), 4633–4642.

Ordaz, A., Oliveira, C. S., Aguilar, R., Carrión, M., Ferreira, E. C., Alves, M., & Thalasso, F. (2008). Kinetic and stoichiometric parameters estimation in a nitrifying bubble column through "in-situ" pulse respirometry. *Biotechnology and Bioengineering*, *100*(1), 94–102.

Pai, T.-Y., Wan, T.-J., Tsai, Y.-P., Tzeng, C.-J., Chu, H.-H., Tsai, Y.-S., & Lin, C.-Y. (2010). Effect of sludge retention time on nitrifiers' biomass and kinetics in an anaerobic/oxic process. *CLEAN - Soil, Air, Water*, *38*(2), 167–172.

Picioreanu, C., Pérez, J., & van Loosdrecht, M. C. M. (2016). Impact of cell cluster size on apparent half-saturation coefficients for oxygen in nitrifying sludge and biofilms. *Water Research*, *106*, 371–382.

Sanchez, O., Marti, M. C., Aspe, E., & Roeckel, M. (2001). Nitrification rates in a saline medium at different dissolved oxygen concentrations. *Biotechnology Letters*, 23, 1597-1602

Shaw, A., *Investigating the Significance of Half-Saturation Coefficients on Wastewater Treatment Processes.* PhD Dissertation, Illinois Institute of Technology. 2015.

Torretta, V., Ragazzi, M., Trulli, E., De Feo, G., Urbini, G., Raboni, M., & Rada, E. (2014). Assessment of Biological Kinetics in a conventional municipal wwtp by means of the oxygen uptake rate method. *Sustainability*, *6*(4), 1833–1847.

Val del Rio, A., Campos, J. L., Da Silva, C., Pedrouso, A., & Mosquera-Corral, A. (2019). Determination of the intrinsic kinetic parameters of ammonia-oxidizing and nitrite-oxidizing bacteria in granular and flocculent sludge. *Separation and Purification Technology*, *213*, 571–577.

van Loosdrecht, M. C. M., Nielson, P. H., Lopez-Vasquez, C. M., & Brdjanovic, D. (2016). *Experimental methods in wastewater treatment*. IWA Publishing.

Wen, J., LeChevallier, M. W., & Tao, W. (2020). Nitrification kinetics and microbial communities of Activated sludge as a Full-scale Membrane Bioreactor plant transitioned to low dissolved Oxygen operation. Journal of Cleaner Production, 252, 119872.

3. Materials and Methods

Experimental setup

The batch tests within this work were conducted using essentially the same experimental setup. The reactors used were 5-liter cylindrical containers with tight-fitting, floating foam covers to limit surface aeration. Surface aeration was assumed to be negligible using this experimental setup and therefore was not considered in analysis. The reactors were mixed using Cole-Parmer® (Vernon Hills, IL) Ultra-Compact Digital Mixers, and pH control was achieved using Cole-Parmer® Alpha pH 560 controller with Cole-Parmer® Tuff-Tip, Semi-Domed 1" Submersible electrode. A pH range of 6.9-7.3 was maintained through the addition of sodium bicarbonate ($NaHCO_3$) and 3% hydrochloric acid (HCl) as needed. Oxygen was supplied to the reactor using

a Schego® (Offenbach, Germany) M2K3 Air Pump through an air stone. Dissolved oxygen within the reactor was measured using PyroScience® (Aachen, Germany) OXROB10 Robust Oxygen Probe, connected to a PyroScience® FireSting-O_2 two-channel meter. The meter was connected to a computer running data acquisition software provided by PyroScience®. An external temperature probe (PyroScience® Pt100) was inserted into the reactor to automatically correct DO readings for slight temperature variations. Ammonia and nitrite substrates were supplied to the reactor using 10,000 mg/L NH_3-N and 10,000 mg/L NO_2^--N stock solutions, respectively. All ammonia, nitrite, and nitrate concentrations were measured by filtering sample through 0.45 µm filter and using Hach (Loveland, CO) TNTplus Vial Tests. A diagram representing the experimental setup as described can be seen in Figure 3 below:

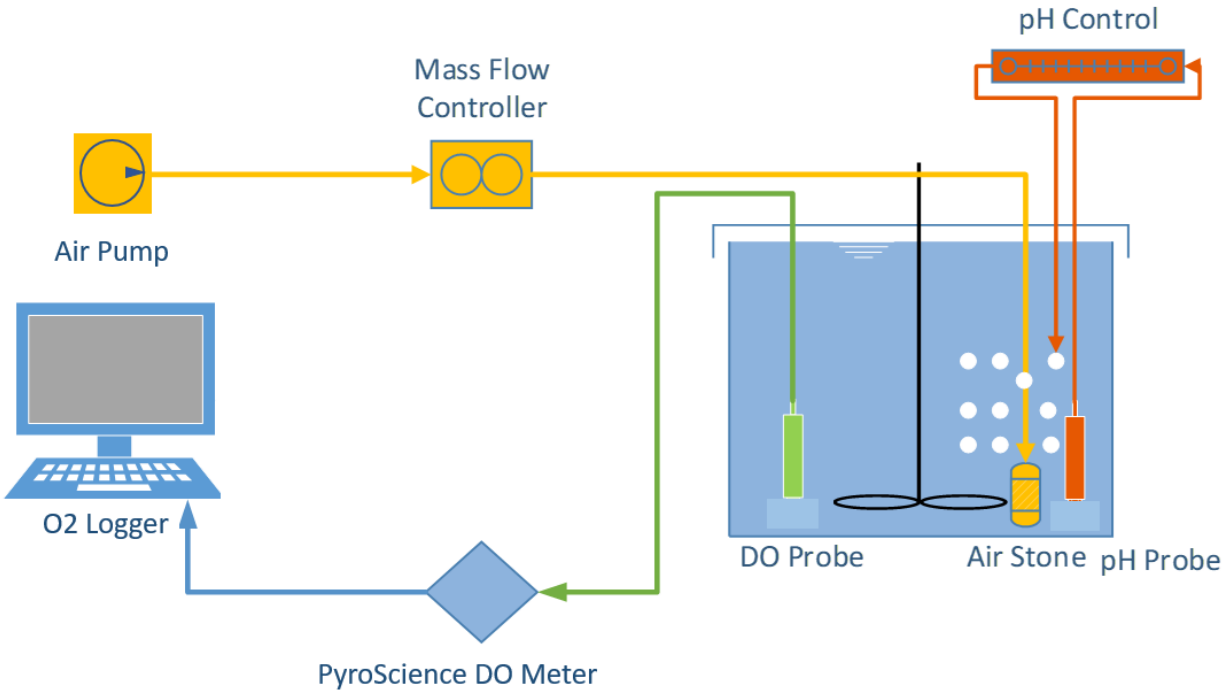

Figure 3. Experimental setup for all batch test procedures within this work.

Initial setup for batch test experiments began by collecting 4-liters of fresh biomass sample, typically obtained from the aeration basin of full-scale WWTPs. The biomass was placed into a reactor and aerated vigorously overnight to confidently establish endogenous conditions. Aerating for upwards of 18-20 hours with mixing and pH control in place also allowed the biomass to acclimate to ambient temperatures within the lab. Reactor temperatures typically ranged between 19-21 °C for all experiments. The DO Probe was calibrated through two-point calibration by establishing saturation and zero points using water aerated to saturation and zero DO water (sodium sulfite, concentration of 20 g/Liter of clean water), respectively. After calibration, the DO probe was positioned into the bulk solution and data collection was initiated. Finally, a tight-fitting floating foam cover was placed atop the reactor.

Declining DO Experimental Procedure

The declining DO batch test consisted of three distinct phases: "endogenous" phase, "nitrite" phase, and "ammonia + nitrite" phase. Each phase began by aerating the reactor to some high DO concentration (typically at least 6 mg O_2/L), removing aeration, and observing DO depletion to zero. A single depletion curve was called a "run". A single run was performed in the endogenous phase, whereas two duplicate runs were performed for the nitrite and ammonia + nitrite phases. Duplicate runs were conducted to provide additional data to analyze for each test. In the nitrite phase, nitrite was always present in non-limiting concentrations. In the ammonia + nitrite phase, both ammonia and nitrite were present in non-limiting concentrations. Substrate concentrations were measured at the beginning and end of each run to ensure at no point was any substrate limiting when it shouldn't be. DO data within the reactor was collected at a frequency of 1/s throughout the entirety of the test.

The purpose of this test design is to isolate each biological functional group: heterotrophic bacteria primarily responsible for endogenous respiration, NOB, and AOB. To avoid potentially inhibitory conditions due to nitrite within the system, concentrations were never higher than 6 mg/L NO_2^--N throughout the test. With nitrite present in the second phase, conventional nitrification pathways dictate that the oxygen uptake rate (OUR) increase compared to the endogenous phase can be attributed to NOB activity. Similarly, with ammonia present in the third phase, the resulting OUR increase compared to the previous phase can be attributed to AOB activity. This test design provided the ability to observe relative oxygen kinetics of nitrifiers without the use of inhibitors. By eliminating the use of inhibitors, biomass conditions representative of full-scale facilities were maintained throughout the test.

Declining DO - Forward Modeling

The declining DO batch test data was analyzed using R computing software. An R script was developed which allowed test data to be imported and easily analyzed for each test. The experimental data was imported as a .CSV file containing two columns: time in first column and DO in second column. Monod functions in terms of OUR (eqn. 4) were used for curve fitting, therefore the experimental data required conversion into terms of OUR. This was accomplished by differentiating measured DO concentration with respect to time. The reaeration portions of the test were not relevant for analysis, and therefore were eliminated from the data. To accomplish this, each run of the test was isolated into its own individual data set, resulting in a total of five data sets: END, NO2-1, NO2-2, NH3-1, and NH3-2. With the relevant OUR data isolated, a forward model was developed which used a system of Monod equations to fit curves to each run of the experiment. This system of equations (10a-10e) is shown below:

$$OUR_{END} = OUR_{END}^{max} * \frac{DO_{END}}{K_{O,END}+DO_{END}} \quad (10a)$$

$$OUR_{NO2\_1} = OUR_{END}^{max} * \frac{DO_{NO2\_1}}{K_{O,END}+DO_{NO2\_1}} + OUR_{NOB}^{max} * \frac{DO_{NO2\_1}}{K_{O,NOB}+DO_{NO2\_1}} \quad (10b)$$

$$OUR_{NO2\_2} = OUR_{END}^{max} * \frac{DO_{NO2\_2}}{K_{O,END}+DO_{NO2\_2}} + OUR_{NOB}^{max} * \frac{DO_{NO2\_2}}{K_{O,NOB}+DO_{NO2\_2}} \quad (10c)$$

$$OUR_{NH3\_1} = OUR_{END}^{max} * \frac{DO_{NH3\_1}}{K_{O,END}+DO_{NH3\_1}} + OUR_{NOB}^{max} * \frac{DO_{NH3\_1}}{K_{O,NOB}+DO_{NH3\_1}} + OUR_{AOB}^{max} * \frac{DO_{NH3\_1}}{K_{O,AOB}+DO_{NH3\_1}} \quad (10d)$$

$$OUR_{NH3\_1} = OUR_{END}^{max} * \frac{DO_{NH3\_2}}{K_{O,END}+DO_{NH3\_2}} + OUR_{NOB}^{max} * \frac{DO_{NH3\_2}}{K_{O,NOB}+DO_{NH3\_2}} + OUR_{AOB}^{max} * \frac{DO_{NH3\_2}}{K_{O,AOB}+DO_{NH3\_2}} \quad (10e)$$

Within this system of equations, each functional group considered in this test is represented by a single Monod term. Each Monod term contains parameters representing the maximum OUR and oxygen half-saturation values for its respective functional group. The parameters in equations 10a-10e are colored to illustrate the functional group's oxygen kinetics represented within each Monod term; green represents endogenous, blue represents NOB, and red represents AOB. This results in a total of six individual parameters within the forward model that were solved to optimize the curve fits over the entire experimental data set simultaneously. A summary of the six parameters used within the forward model can be found in Table 4.

Table 4. Oxygen kinetic parameters solved within the forward model

P[1]	OUR_{END}^{max}
P[2]	$K_{O,END}$
P[3]	OUR_{NOB}^{max}
P[4]	$K_{O,NOB}$
P[5]	OUR_{AOB}^{max}
P[6]	$K_{O,AOB}$

A residual function was used to quantify the difference between the measured OUR data and the Monod curves created by the system of equations within the forward model:

$$OUR_{measured} - OUR_{fit} \quad (11)$$

The difference between the measured OUR and Monod curves created in the forward model was minimized by finding the optimum values for each of the six parameters summarized in Table 4. A native R operation called "modFit" was used to minimize the result of the residual function by solving for optimum values for each parameter within the forward model. The modFit function required initial guesses for each of the six parameters. Experimenting with a variety of initial guesses for parameter values yielded consistent results, therefore it was concluded that the modFit function was not sensitive to initial guess values within this analysis. There were a variety of minimization methods to choose from that can be used by modFit to solve for optimum parameter values. Some examples of minimization methods included:

Levenberg-Marquardt ("Marq"), Nelder-Mead, Broyden-Fletcher-Goldfarb-Shanno ("BFGS"), and Pseudorandom algorithm ("Pseudo"). Experimenting with a variety of minimization methods was found to have little effect on the final solution, therefore the Levenberg-Marquardt algorithm (the default minimization method) was selected for this step in the analysis.

The significance of this curve fitting analysis is that it is not being conducted for each individual set of experimental OUR data, but rather across the entire data set simultaneously. This means that the oxygen kinetics for each functional group were being considered throughout the fitting analysis. For instance, the parameters representing endogenous respiration were not only being solved for within the endogenous phase, as they are present throughout the entirety of the test. Therefore, the endogenous parameters were included in each Monod function within the system of equations developed in the forward model. Using this strategy, it was possible to distinctly measure the oxygen half-saturation of each functional group without altering the characteristics of the wastewater, providing a more accurate representation of the oxygen kinetics within a full-scale treatment facility.

Statistical Proof - Inverse Modelling

The validity of the optimum values for oxygen kinetic parameters obtained in the forward model was assessed using an inverse model based on Bayesian statistics. Bayesian statistics are based on Bayes' theorem, which combines prior knowledge regarding parameter values with information gained from observed data. This combination of observed and modelled data yields a final distribution of values, called the posterior distribution, which represents a range of potential values for any given parameter within the forward model (van de Schmoot et al. 2021).

The specific method of Bayesian statistics applied to this work is called the Markov chain Monte Carlo (MCMC) method. The MCMC method is designed to be applied to nonlinear models, which takes into consideration both the uncertainty in the parameters from the forward model as well as the final output values (Soetaert & Petzoldt, 2010). The strategy of this method is to input a very large number of sets of parameters into the forward model and assess the variance of the outcome. If the variance is below a desired threshold, the model run is accepted. Each iteration of parameters used by the inverse model is based on the previous input adjusted by a specified value called the "jump" parameter. This jump value influences what percentage of runs produce an accepted outcome. A jump value too large or too small can result in an incomplete exploration of the state space for potential parameter inputs into the model. Literature states that the optimal acceptance rate is 0.234, or 23.4% of accepted outcomes from the MCMC process (Roberts et al. 1997). For this study, acceptance rates of 20-25% were targeted.

The inverse model process began by conducting a pilot MCMC simulation with the minimum number of iterations required to run a Raftery and Lewis diagnostic (3746 iterations). The

purpose of this diagnostic was to estimate the minimum number of iterations required to achieve a specified level of precision for the MCMC output i.e., 95% confidence on the parameter output (Raftery & Lewis, 1995). The full MCMC simulation was conducted using a significantly higher number of iterations than the required minimum for 95% confidence. The number of iterations used within this work was 100,000. Two separate MCMC simulations were conducted to ensure the models behaviors were consistent. A check for convergence between the two MCMC simulations was performed using the Gelman Statistic, which gives additional indication that the simulations behaved in a similar way. The Gelman statistic outputs a list containing estimates of the potential scale reduction factor, or shrink factor, for each of the six parameters tested in the inverse model.

The most important output of the Gelman statistic is a single value called the multivariate potential scale reduction factor (PSRF), which should be below 1.1 and as close to 1.0 as possible. A multivariate PSRF value of 1.0 indicates there is no variance between the two simulations (Brooks, 1998). For all declining DO tests analyzed using this procedure, a multivariate PSRF value of 1.0 (or very close to 1.0) was always achieved. The final output of the combined MCMC simulation includes mean and standard deviation values for the parameters tested as well as 2.5%, 25%, 50%, 75%, and 97.5% quantiles. With the summarized results from the MCMC analysis completed, the resulting mean and quantile values were used to plot the final estimation for OUR Monod curves for both NOB and AOB.

Experimental Setup - Substrate Utilization Rate Test

The oxygen half-saturation results from the declining DO test method were assessed by comparing the results obtained from the substrate utilization rate test. These tests were performed in parallel using identical experimental setups. The experimental setup for the substrate utilization rate test included the use of a Cole-Parmer® Precision Mass Flow Controller (0-5 Standard liters Per Minute (SLPM)) to precisely control oxygen input and establish various DO setpoints throughout the test. This test was designed to measure NOB and AOB activity rates as a function of DO concentration. At each DO setpoint, nitrogen species (NH_3, NO_2^-, and NO_3) concentrations were measured at ten-minute intervals. NOB activity was estimated by calculating the slope associated with the change in nitrate concentration over time. Assuming any denitrification occurring within the reactor is negligible, measured change in NO_3 (NO_3 production rate) concentration within the reactor can be attributed to nitratation by NOB (equation 12). AOB activity was estimated by calculating the slope associated with the change in NO_X (NO_2^- + NO_3) over time for each DO setpoint. Once again, assuming denitrification rates to be negligible, the measured change in NO_X concentration (NO_X production rate) within the reactor can be attributed to nitritation by AOB (equation 13).

$$NUR = \Delta NO_3 \tag{12}$$

$$AUR = \Delta NO_X \tag{13}$$

NOB and AOB activity rates (nitrite uptake rate (NUR) and ammonia uptake rate (AUR), respectively) determined at a range of DO concentrations were plotted versus DO. Best fit Monod curves for both NOB and AOB were determined using squared sum error (SSE) method in Microsoft Excel by solving for optimum values of maximum utilization rate and oxygen half saturation.

Full-Scale Wastewater Treatment Facility Overview

Declining DO & substrate utilization rate parallel batch tests were conducted using biomass samples collected from several full-scale HRSD wastewater treatment facilities. Summaries for operating conditions at each of these facilities are provided in Table 5:

Table 5. Summary of wastewater operating conditions at HRSD's Virginia Initiative Plant (VIP), Army Base Treatment Plant (ABTP), and King William Treatment Plant (KWTP)

	Average DO (mgO_2/L)	Average SRT (days)	Average Floc Size (µm)
VIP	1.1	11	60
ABTP	0.9	12	160
KWTP	4.9	48	>5

Both VIP and ABTP are BNR activated sludge treatment facilities utilizing the patented VIP process and 5-stage Bardenpho biological nutrient removal systems, respectively. Average daily flows for VIP and ABTP are 40 MGD and 18 MGD, respectively. KWTP is a 4-stage Bardenpho system with membrane bioreactor (MBR) treatment facility, treating a much smaller average daily flow of 0.1 MGD.

4. Results & Discussion

DO Probe Response Time

Correcting for the probe response time was investigated to observe whether it had a significant effect on the outcome of the results for the declining DO analysis. This was performed using procedure previously described by Guisasola et al. (2005). The probe response time (t95) was estimated by quickly switching DO probe between water at saturation and zero DO water (using sodium sulfite) and found to be approximately 7 seconds (figure provided in Appendix). The measured DO values were corrected using equation 8, where τ = 7 seconds and Δt (data collection frequency) = 1/s. Both corrected and uncorrected DO measurements for a declining DO test were carried through the described forward and inverse model analysis, yielding the results summarized in Table 6.

Table 6. Comparison of K_O results determined through forward and reverse modelling for uncorrected and corrected measured DO data (95% IQR)

	$K_{O,NOB}$ (mg O_2/L)	$K_{O,AOB}$ (mg O_2/L)
Uncorrected	0.203 ± 0.021	0.671 ± 0.028
Corrected	0.202 ± 0.022	0.672 ± 0.031

This analysis required a sensitive probe with high data collection frequency and fast response time to accurately measure DO changes at low concentrations. Equation 8 corrected the measured DO data using the probe performance characteristics and was found to have little effect on the results for $K_{O,NOB}$ and $K_{O,AOB}$. Using a highly sensitive DO probe with a fast response time as well has a high data collection frequency provided the ability to use the measured DO data to accurately perform the declining DO analysis as described.

Declining DO Results

The following results were obtained from a declining DO test conducted in parallel with a substrate utilization rate test performed using VIP biomass on August 17th, 2021. Figure 4 shows the experimental DO data collected using PyroScience® DO probe and data acquisition software.

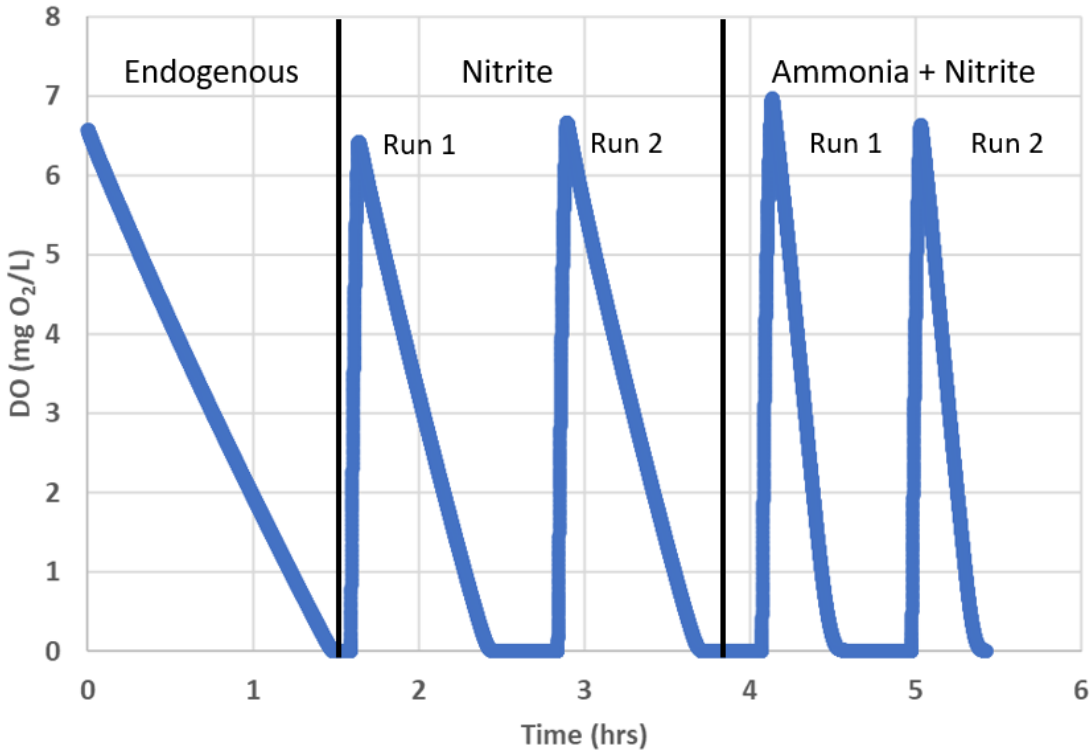

Figure 4. Declining DO batch test results (VIP, 8-17-21) with dissolved oxygen (mg O2/L) on the Y-axis and time (hours) on the X-axis. Data points collected using PyroScience O_2 Logger were exported and plotted in Microsoft Excel.

From the experimental DO data, OUR data was created for each run of the declining DO test by differentiating DO with respect to time in R. A collection of the resulting OUR curves for each phase of the test can be seen in Figure 5.

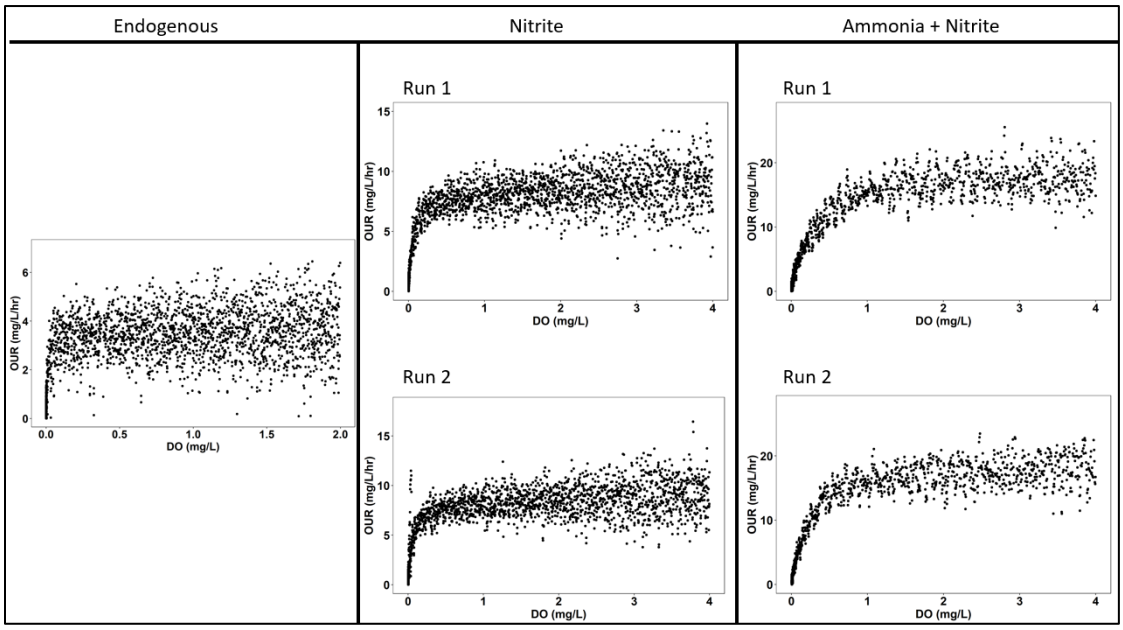

Figure 5. Experimental OUR data for each phase and run of declining DO test.

The OUR data is supplied to the forward model which creates Monod curves using the system of equations 10a-10e. Results of optimum oxygen kinetic parameter values determined in the forward model are summarized in Table 7:

Table 7. Optimized estimates for parameters in forward model using R minimization methods.

Parameter	Estimate	Standard Error
OUR_{END}^{max}	3.69 mg O_2/L/hr	0.046
$K_{O,END}$	0.04 mg O_2/L	0.003
OUR_{NOB}^{max}	5.91 mg O_2/L/hr	0.066
$K_{O,NOB}$	0.26 mg O_2/L	0.015
OUR_{AOB}^{max}	9.66 mg O_2/L/hr	0.099
$K_{O,AOB}$	0.42 mg O_2/L	0.022

Using the optimized oxygen kinetic parameter values obtained through the forward model, the resulting Monod curves were plotted over the experimental OUR data to observe the effectiveness of the fits, shown with associated K_O values in Figure 6:

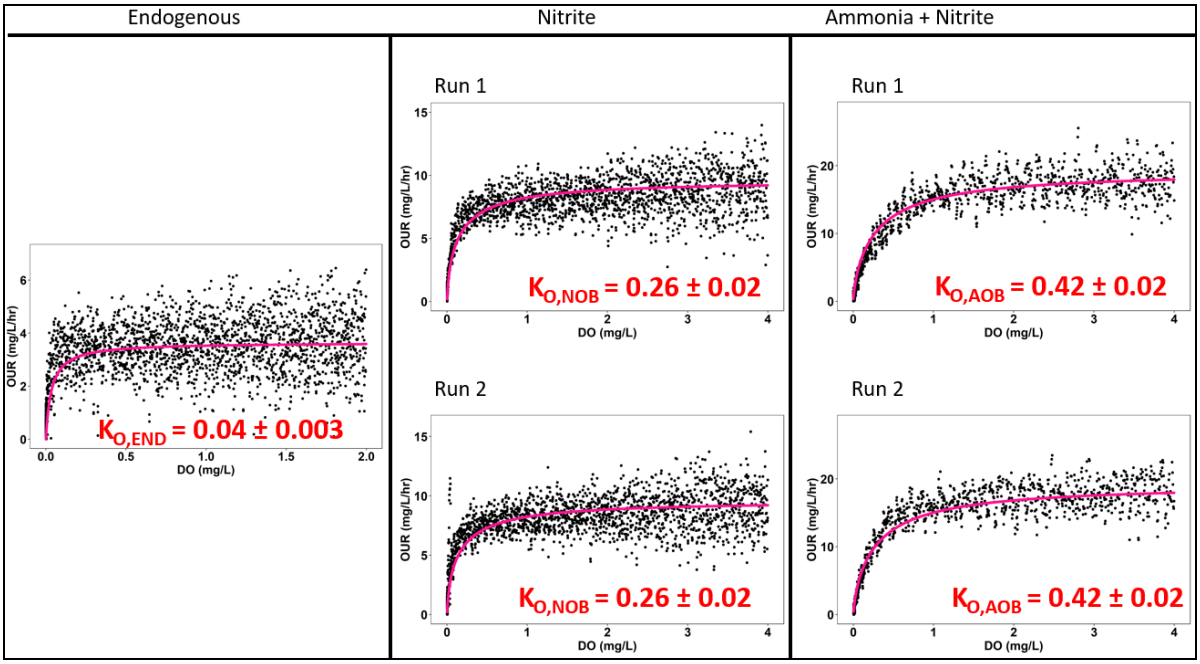

Figure 6. OUR curve fits for each run of experimental OUR data after parameter optimization in forward model.

The validity of the optimized oxygen kinetic parameter values obtained through the forward model was assessed using the inverse model. The MCMC simulations carried out by the inverse model provided mean, standard deviation, and quantile values for each parameter estimated within the forward model. The results of the inverse model are summarized in Tables 8 and 9:

Table 8. Mean and standard deviation value results from combined MCMC inverse model

Parameter	Mean	Standard Deviation
OUR_{END}^{max}	3.89 mg O_2/L/hr	0.050
$K_{O,END}$	0.06 mg O_2/L	0.005
OUR_{NOB}^{max}	5.62 mg O_2/L/hr	0.066
$K_{O,NOB}$	0.22 mg O_2/L	0.013
OUR_{AOB}^{max}	9.66 mg O_2/L/hr	0.088
$K_{O,AOB}$	0.42 mg O_2/L	0.019

Table 9. Quantile results from combined MCMC inverse model

Parameter	2.5%	25%	50%	75%	97.5%
OUR_{END}^{max}	3.80	3.86	3.89	3.93	3.99
$K_{O,END}$	0.061	0.066	0.069	0.073	0.079
OUR_{NOB}^{max}	5.49	5.58	5.62	5.67	5.75
$K_{O,NOB}$	0.18	0.20	0.21	0.21	0.23
OUR_{AOB}^{max}	9.49	9.60	9.66	9.72	9.83
$K_{O,AOB}$	0.39	0.41	0.42	0.44	0.46

The quantile results in Table 8 can be used to develop an interquartile range (IQR) for any desired range. A 95% IQR was used within this work (2.5% quantile - 97.5% quantile). The results obtained from the inverse model using MCMC analysis for both NOB and AOB are plotted in Figures 7 and 8:

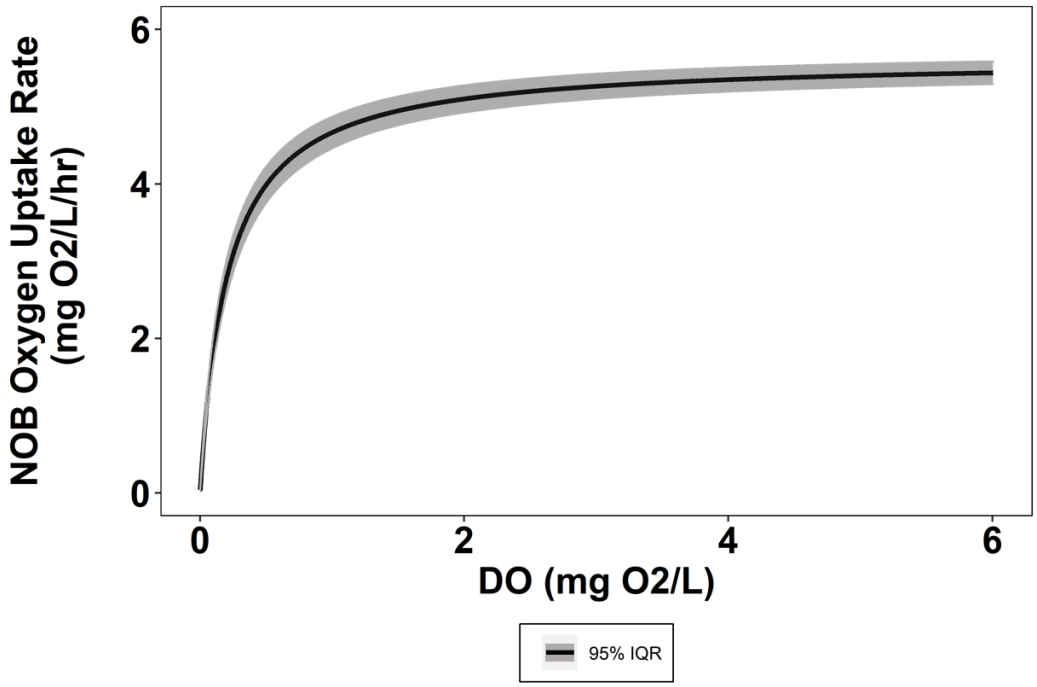

Figure 7. Final average OUR curve with 95% IQR representing NOB oxygen kinetics from declining DO test using forward and inverse modelling with MCMC analysis.

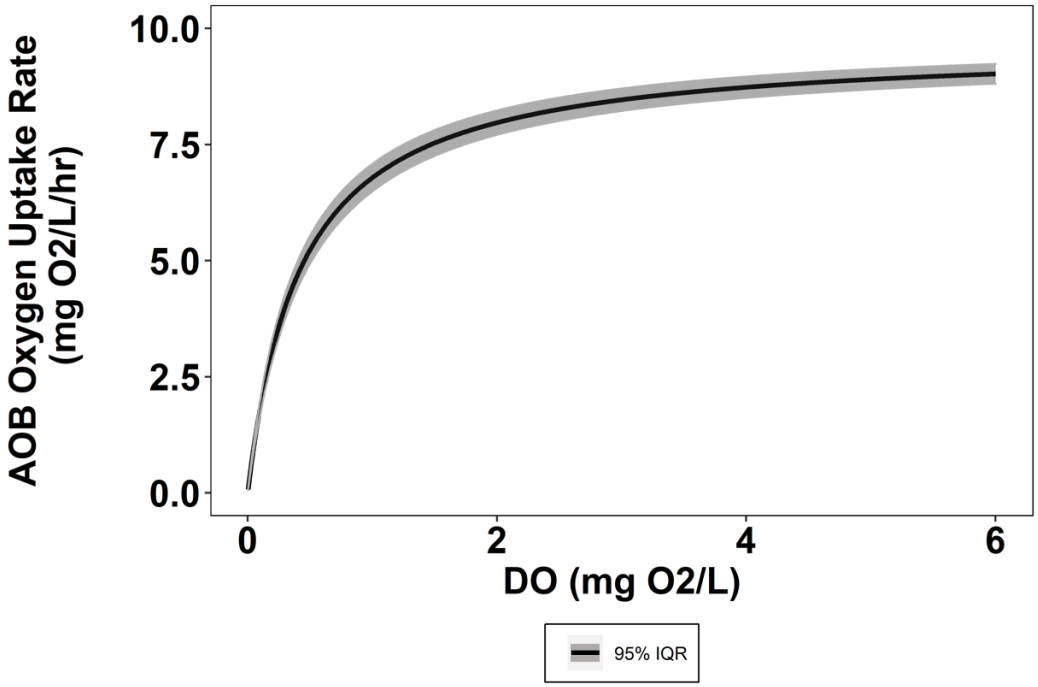

Figure 8. Final average OUR curve with 95% IQR representing AOB oxygen kinetics from declining DO test using forward and inverse modelling with MCMC analysis.

Figures 7 and 8 represent the final results from the declining DO testing method and analysis, which describe NOB and AOB OUR curves for a range of DO concentrations from 0 – 6 mg O_2/L. Using these figures, one could estimate with 95% confidence how nitrifiers will perform when exposed to any DO concentration for a short period of time. These results suggest NOB can maintain OURs close to their observed max at lower DO concentrations relative to AOB. This relationship was maintained in all tests, where $K_{O,NOB}$ was always observed to be lower than $K_{O,AOB}$.

Substrate Utilization Rate Results

The following results were obtained from the substrate utilization rate test conducted in parallel with the declining DO test performed using VIP biomass on August 17th, 2021. Figure 13 shows the experimental data collected in this test.

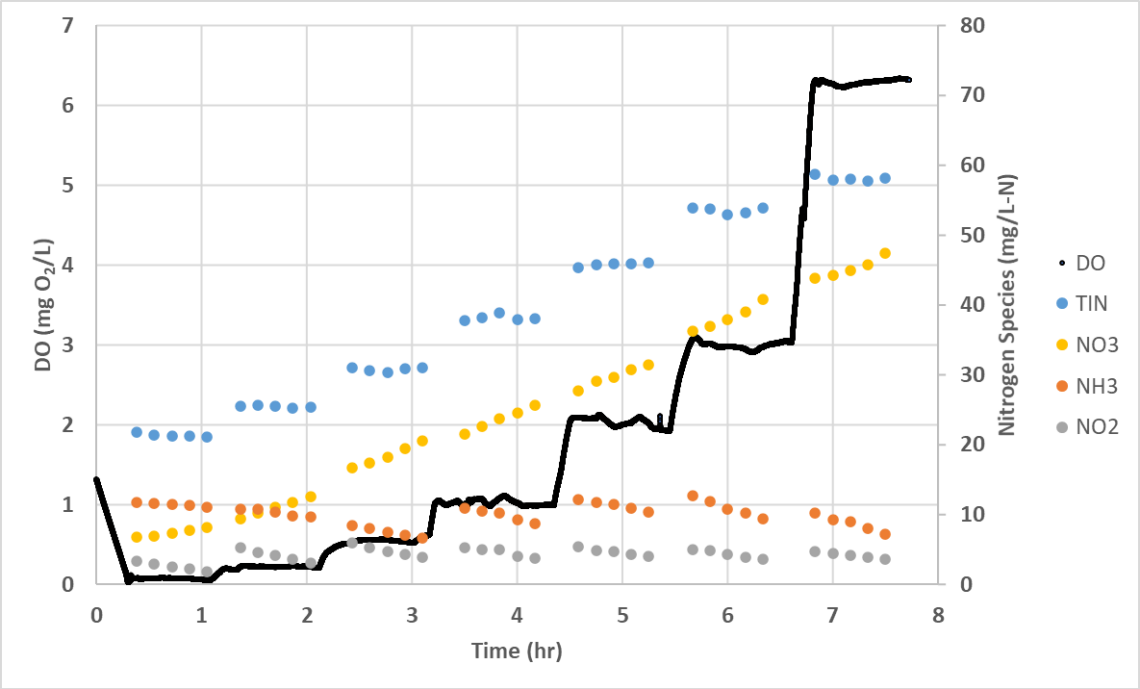

Figure 9. Substrate utilization rate batch test results (VIP. 8-17-21), where dissolved oxygen (mg O_2/L) on the primary Y-axis, nitrogen species (mg/L-N) on the secondary Y-axis, and time (hours) on the X-axis. Data points collected using PyroScience O_2 Logger were exported and plotted in Microsoft Excel.

Nitrite uptake rates (NUR) and ammonia uptake rates (AUR) were determined for NOB and AOB, respectively, using equations 12 and 13 at each DO setpoint. A summary for substrate utilization rates is shown in Table 10.

Table 10. Summary of substrate utilization rates for NOB and AOB determined in 8-17-21 VIP parallel test

DO Setpoint (mg O_2/L)	NUR (mg NO_2^-/L/hr)	AUR (mg NH_3/L/hr)
0.07	2.21	0.09
0.22	4.63	1.42
0.55	5.76	2.82
1.0	6.06	3.61
2.0	5.52	3.56
3.0	6.72	4.54
6.0	5.28	3.51

Best fit curves to the experimentally determined NUR and AUR data were developed using the SSE method, shown in Figures 10 and 11:

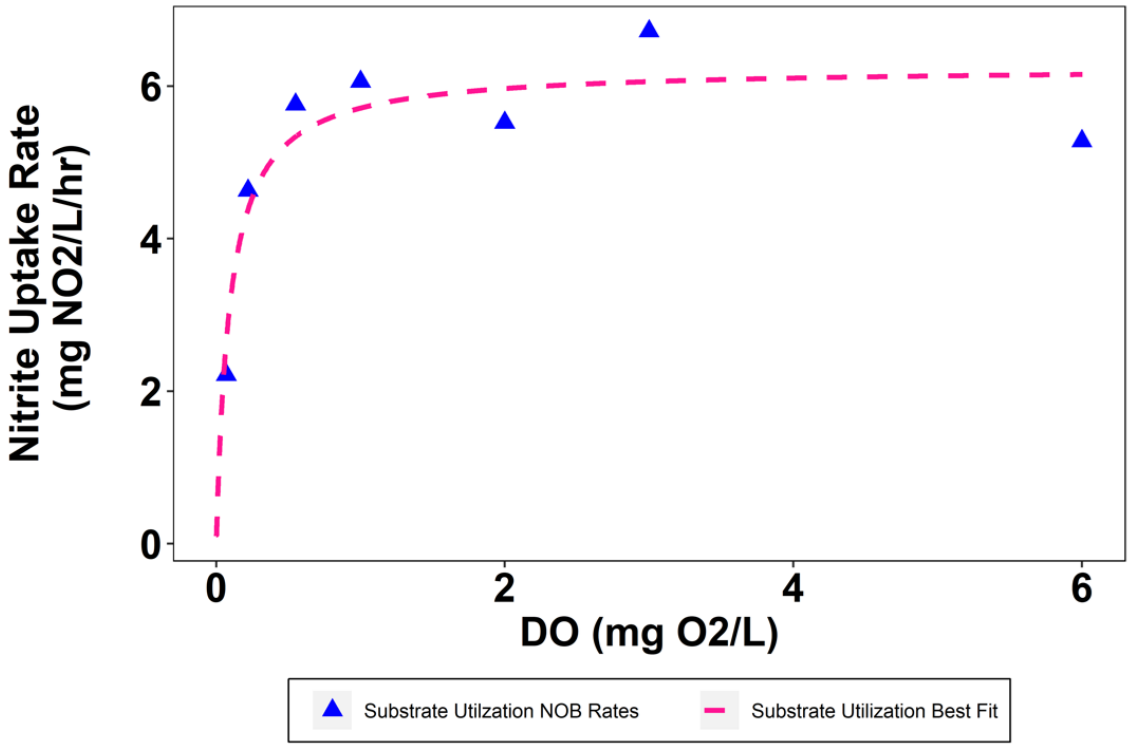

Figure 10. NUR vs DO for substrate utilization rate test. NUR_{max} = 6.25 (mg NO_2^-/L/hr) and $K_{O,NOB}$ = 0.09 (mg O_2/L) determined using SSE method.

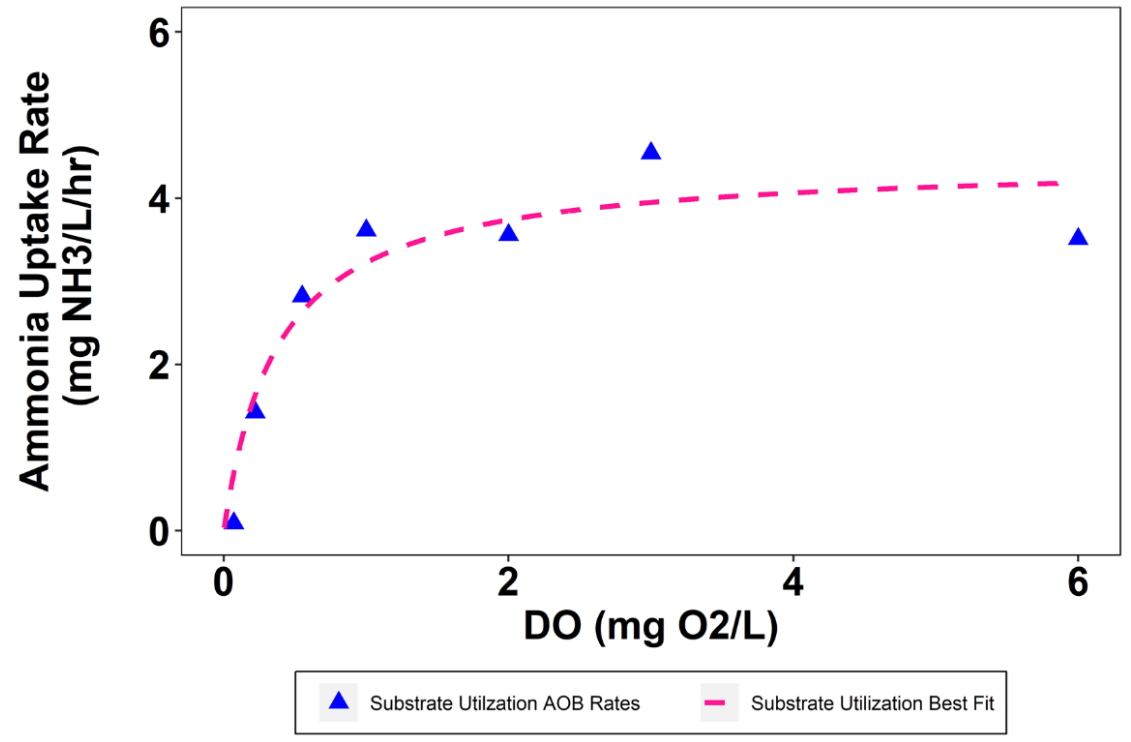

Figure 11. AUR vs DO for substrate utilization rate test. AUR_{max} = 4.45 (mg NH3/L/hr) and $K_{O,AOB}$ = 0.38 (mg O2/L) determined using SSE method.

Like the results observed in figures 7 and 8, NOB and AOB best fit uptake rate curves shown in figures 10 and 11 resulting from the substrate utilization rate test suggest NOB can maintain substrate uptake rates close to their observed max at lower DO concentrations relative to AOB.

Declining DO and Substrate Utilization Rate Methods Comparison

The oxygen half-saturation results for both NOB and AOB obtained from the declining DO test analysis were compared to the values determined from the substrate utilization rate test. The MCMC analysis for the declining DO test provided results in terms of OUR, whereas the results from the substrate utilization rate test were in terms of NUR & AUR. To graphically compare the results from the two test methods, the declining DO OUR results for NOB and AOB were converted into NUR and AUR, respectively. The following stoichiometric equations 14 and 15, which link mass oxygen/mass substrate and nitrifier yield, were used for this conversion (Metcalf & Eddy, 2003):

$$1.14 - Y_{NOB} = \frac{g\ O_2}{g\ NO_2{-}N} \tag{14}$$

$$\frac{3.43 - Y_{AOB}}{1+i_{N,B}*Y_{AOB}} = \frac{g\ O_2}{g\ NH_x{-}N} \tag{15}$$

Where:

Y_{NOB} = NOB Yield (estimated range between 0.09 – 0.25 g COD/g N)
Y_{AOB} = AOB Yield (estimated range between 0.15 – 0.45 g COD/g N)
$i_{N,B}$ = nitrogen content of biomass (0.07 g N / g COD)

Nitrifier yield was not measured within the scope this work, therefore when converting declining DO test results into terms of nutrient uptake rates, a range of yield values were chosen from supporting literature for both NOB and AOB. It is important to note that adjusting the yield value does not change the shape of the resulting curve, only the magnitude. Yield values used in various literature is summarized in Table 11.

Table 11. Nitrifier yield values used within various literature sources

$Y_{,NOB}$ (g COD/g N)	Y_{AOB} (g COD/g N)	Source
0.06	0.20	Liu et al. 2012
0.05	0.21	Fang et al. 2009
0.07	0.14	Blackburne et al. 2007
0.09	0.15	Jones et al. 2007
0.45	0.45	Rittman et al. 1999

After converting the results from the declining DO analysis for NOB and AOB into terms of substrate uptake rates, the results from the two testing methods can be compared graphically, as shown in Figures 12 and 13, respectively:

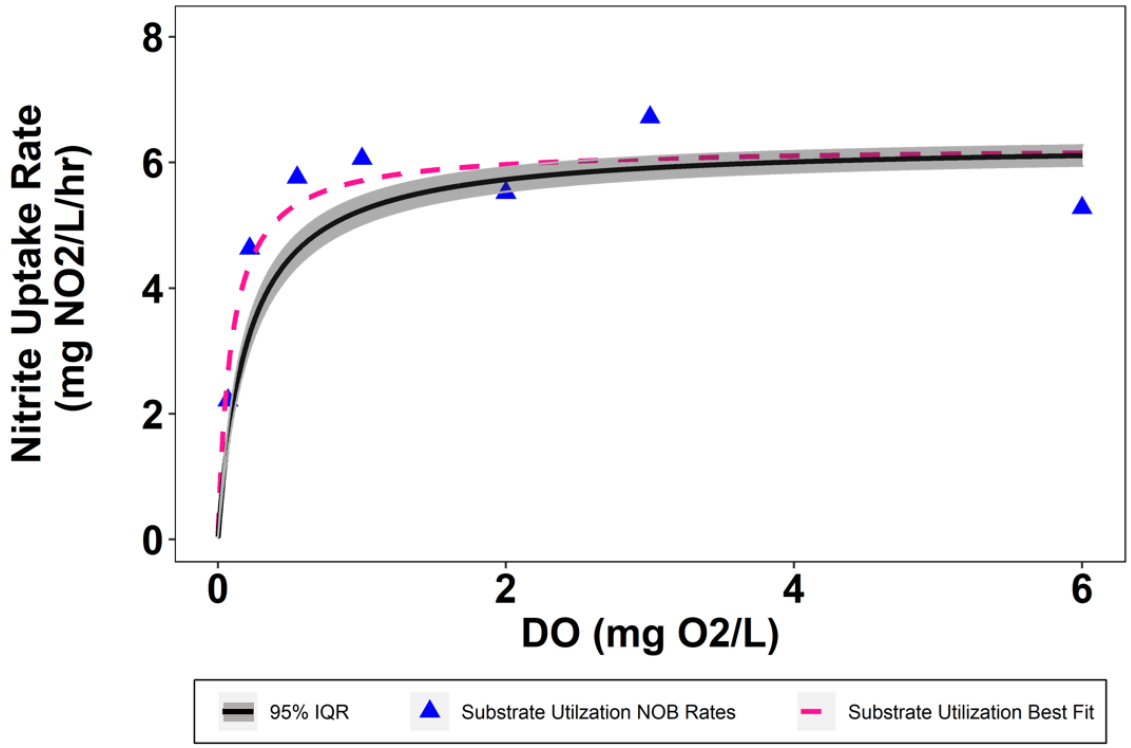

Figure 12. NUR vs. DO results comparison between declining DO and substrate utilization rate batch tests. Y_{NOB} assumed to be 0.25 (g COD/g N).

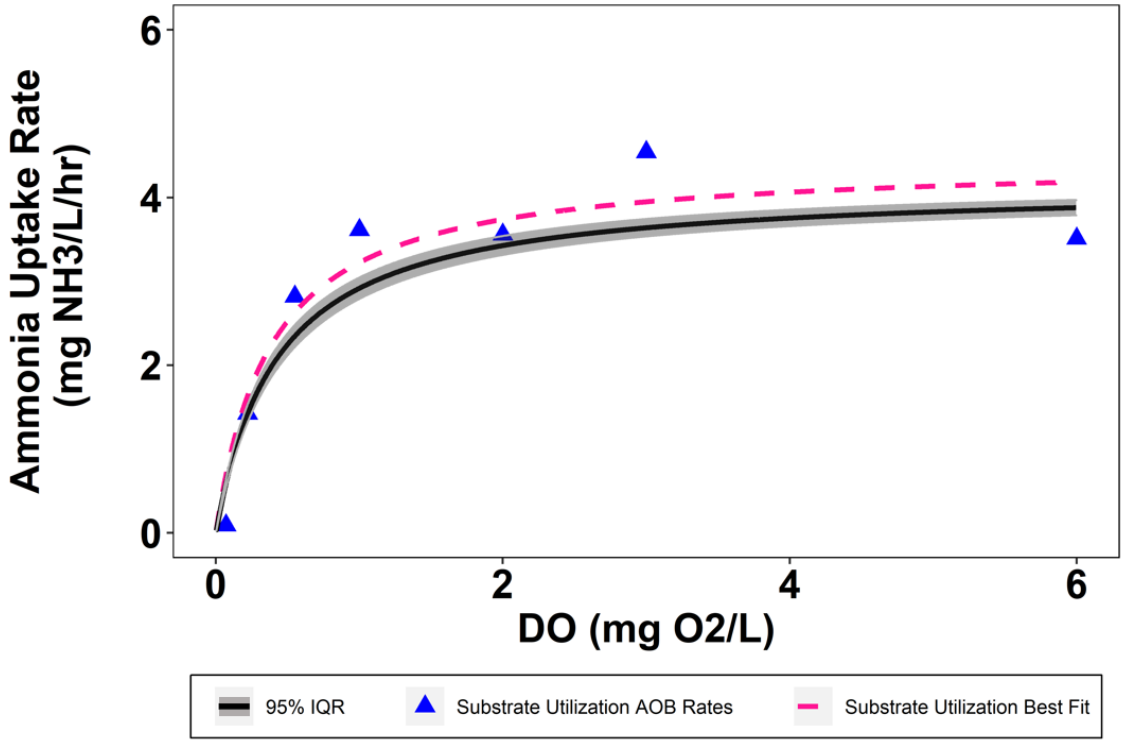

Figure 13. AUR vs. DO results comparison between declining DO and substrate utilization rate batch tests. Y_{AOB} assumed to be 0.45 (g COD/g N)

Parallel Test Results for Oxygen Half-Saturation

The purpose of conducting the declining DO test in parallel with the substate utilization rate test was to observe how the oxygen half-saturation rate results compare between the two testing methods. It was possible to visually compare the consistency between the two tests by plotting the K_O results from the declining DO test on the Y-axis along with the K_O results from the substrate utilization rate test on the X-axis as seen in Figure 14.

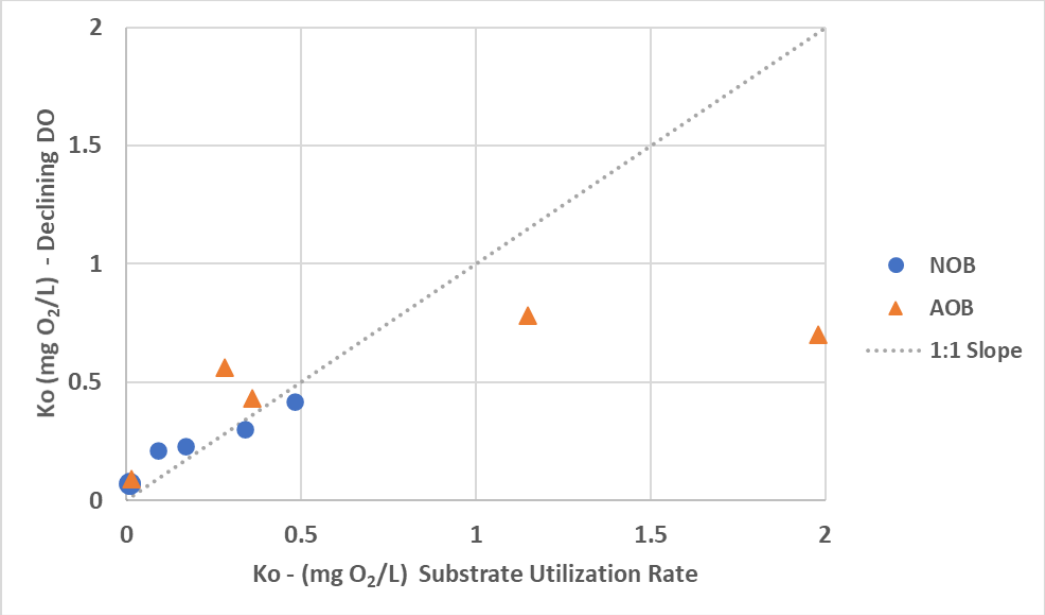

Figure 14. Oxygen half-saturation results from Parallel Tests conducted using biomass samples from VIP, Army Base Treatment Plant, and King William Treatment Plant.

The visual comparison of the K_O values in Figure 14 suggests there is consistency between the oxygen half-saturation results for the two testing methods. The single outlier represents AOB results from ABTP, where the substrate utilization rate test yielded an AOB K_O value of 1.98 mg O_2/L. This value is significantly outside the range of values for CAS within literature (Table 1). The declining DO K_O value was measured to be 0.70 mg O_2/L, which is consistent with AOB values observed throughout all other tests within this study using CAS. The outlier result obtained from the substrate utilization rate test highlights the issue associated with that testing method: with only seven points to which a Monod curve can be fit, any potential error associated with one or more of those points could influence the curve fit greatly. That risk for error could be reduced by estimating substrate uptake rates at additional DO setpoints, however that would require even more time for a testing method that already requires upwards of 8 hours to conduct. Regardless of the potential error associated with the substrate utilization rate test, it was necessary to compare the results obtained using the developed

declining DO method. Table 12 summarizes all K_O results obtained from parallel tests conducted for VIP, ABTP, and KWTP:

Table 12. Summary for all KO results determined from declining DO and substrate utilization rate tests conducted in parallel

		Declining DO (mg O_2/L)	Substrate Utilization Rate (mg O_2/L)
VIP (4/23/21)	$K_{O,NOB}$	0.23	0.17
	$K_{O,AOB}$	0.56	0.28
VIP (4/29/21)	$K_{O,NOB}$	0.30	0.34
	$K_{O,AOB}$	0.85	1.15
VIP (8/17/21)	$K_{O,NOB}$	0.21	0.09
	$K_{O,AOB}$	0.43	0.36
ABTP (5/27/21)	$K_{O,NOB}$	0.42	0.48
	$K_{O,AOB}$	0.70	1.98
KWPT (5/18/21)	$K_{O,NOB}$	0.07	0.01
	$K_{O,AOB}$	0.09	0.02

Observing consistent trends in the K_O results using two different measurement methods indicated with greater confidence that the declining DO method provided accurate results. For both methods, $K_{O,NOB}$ was always observed to be less than $K_{O,AOB}$. The three parallel tests conducted using VIP biomass suggested there was less variability associated with the declining DO method ($K_{O,NOB}$ = 0.21 – 0.30, $K_{O,AOB}$ = 0.43 – 0.85) compared to the substrate utilization rate method ($K_{O,NOB}$ = 0.09 – 0.34, $K_{O,AOB}$ = 0.28 – 1.15). For both NOB and AOB results, the values determined from the declining DO method were within the range of values determined using the substrate utilization rate method. In the case of the KWTP rates, the measured K_O values were lower than the lowest DO setpoint used within the substrate utilization rate test (0.1 mgO_2/L). When performing the substrate utilization rate test on biomass expected to exhibit very low K_O values (i.e., MBR biomass) it would be ideal to use DO setpoints at much lower concentrations. However, it proved difficult to establish various setpoints lower than 0.1 mg O_2/L. In the case of the declining DO method, this was not an issue as the test procedure observed nitrifier performance down to zero DO in all cases. The overall consistency of K_O trends observed between the two methods conducted in parallel provided evidence that the declining DO method can be used to estimate oxygen half-saturation for both NOB and AOB without the use of selective inhibitors.

Full-Scale Operating Conditions Effect on Observed K_O

Average floc size between the three facilities was investigated using a Leica DM 2500 phase contrast microscope and Leica MC170HD camera. Floc photos collected for each treatment

facility are provided in Appendix. With an average floc size established for VIP, ABTP, and KWTP, the Ko values resulting from the declining DO test were compared to the observed average floc size (µm) as shown in Figure 15.

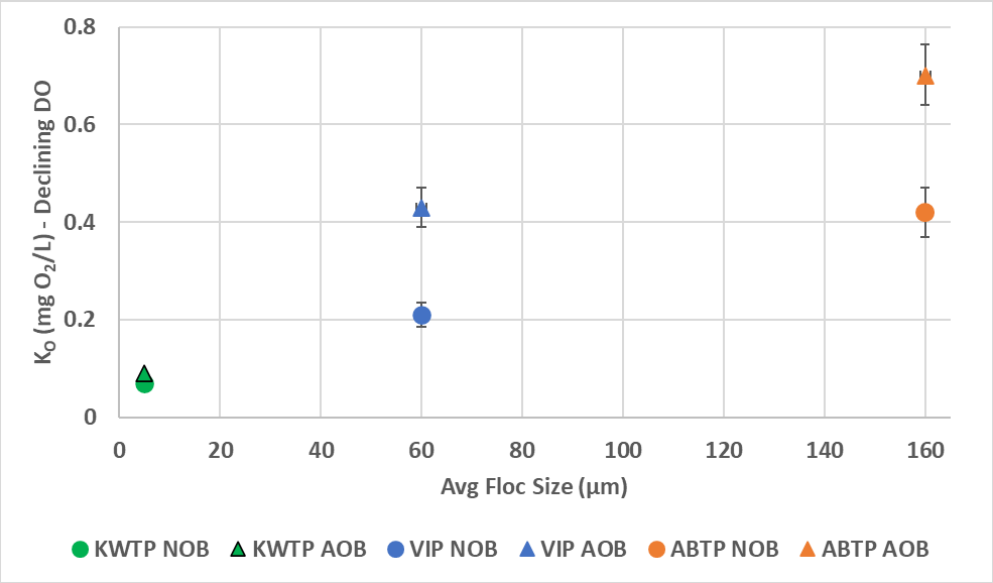

Figure 15. Oxygen half-saturation results from declining DO analysis plotted versus average floc size (µm) with 95% IQR generated from the MCMC analysis.

There appeared to be a strong correlation between average floc size and apparent oxygen half-saturation. Without any selective pressures within the MBR process, very little floc formation keeps average floc size small at KWTP relative to VIP and ABTP. For KWTP, relatively small floc sizes suggest minimal oxygen mass transfer limitation, therefore measured K_O values would be more representative of the intrinsic K_O values. The increasing Ko values measured with VIP and ABTP tests suggest greater oxygen mass transfer limitation due to larger average floc size. Additional floc morphology parameters such as floc density would also have a significant effect on mass transfer limitation, but were not considered within the scope of this work.

An average DO concentration within the aeration tanks for each of these treatment plants was determined for the 30-day period leading up to sample collection and compared to the K_O results from the declining DO test as shown in Figure 16.

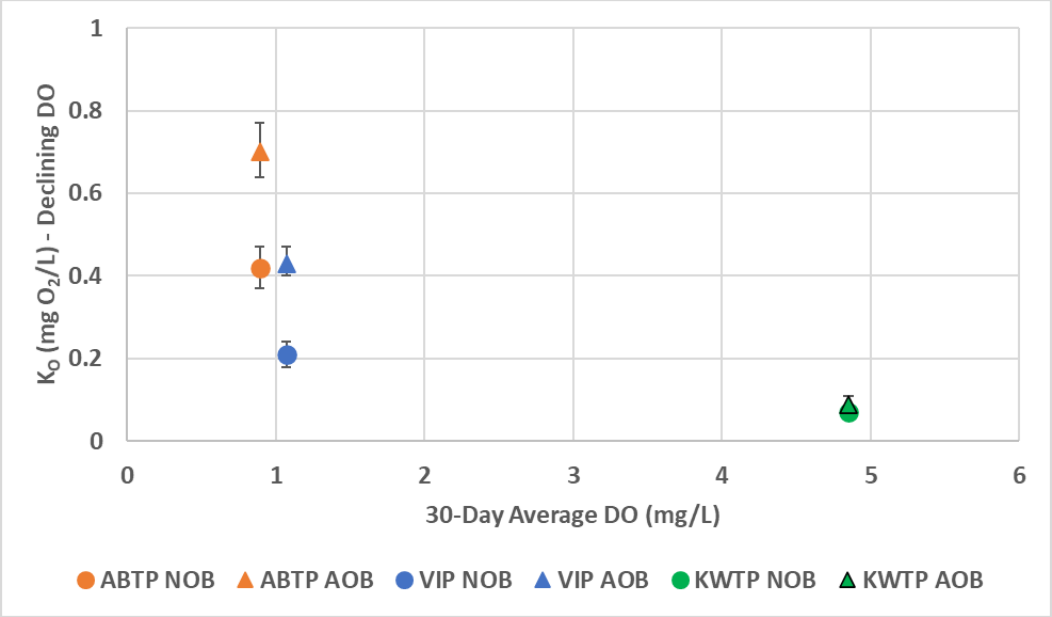

Figure 16. Oxygen half-saturation results from declining DO test versus 30-day average DO concentration with 95% IQR generated from the MCMC analysis.

As with average DO, the average SRT was also considered for the 30-day period leading up to sample collection for each of the parallel tests performed. K_O results determined through the declining DO method were compared to 30-day average SRT as shown in Figure 17.

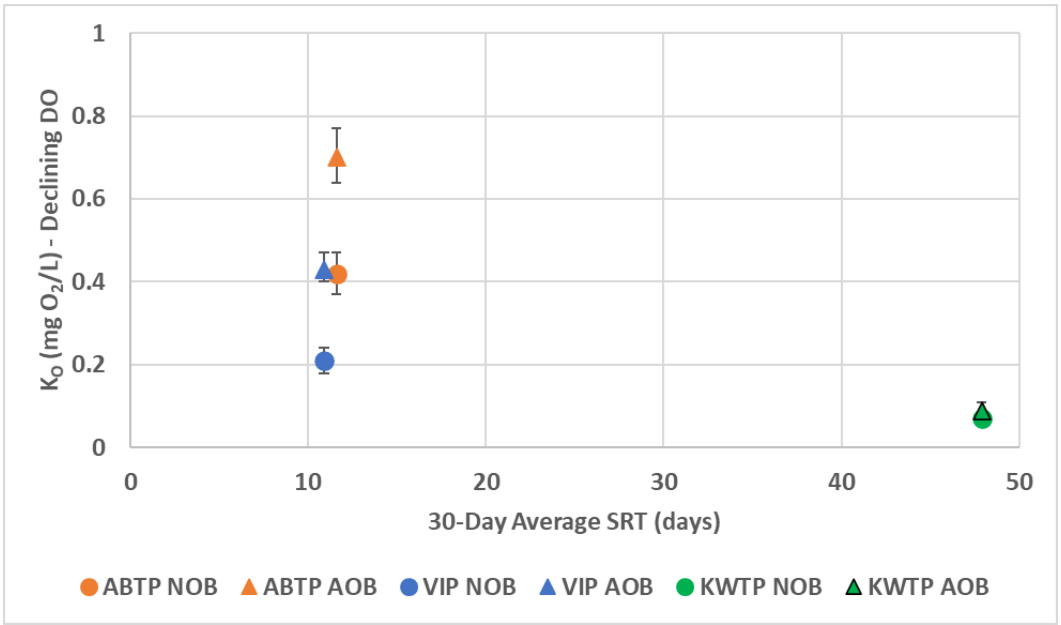

Figure 17. Oxygen half-saturation results from declining DO test versus 30-day average SRT with 95% IQR generated from the MCMC analysis.

Considering potential nitrifier adaptation, nitrifiers exposed to lower average DO conditions were expected to exhibit lower relative observed K_O values, however the results plotted in Figure 16 did not show that relationship. The average DO conditions between the three

facilities in Table 5 suggested that oxygen is largely non-limiting in all cases. This can be assumed based on the observed K_O values for each facility: In all cases, both $K_{O,NOB}$ and $K_{O,AOB}$ were lower than the average DO conditions. Nitrifiers exposed to DO concentrations higher than their apparent K_O suggest they are consuming oxygen (therefore nitrifying) closer to their maximum rate. Unless exposed to DO conditions at or below their apparent K_O values for extended periods of time, nitrifiers are not likely to be experiencing pressure for adaptation. Much like with the average DO conditions, average SRT does not appear to have a strong correlation with apparent K_O values for NOB or AOB. The relationship between average floc size and observed K_O results suggested floc morphology has a greater influence on observed oxygen half-saturation than average SRT and DO conditions between biomasses collected from the three WWTPs considered within this study.

Declining DO Batch Test Results for VIP

Declining DO tests were performed using VIP biomass from April through August 2021. Operational changes to the facility during that time include transitioning from setpoint DO control to ammonia-based aeration control (ABAC) in June. Before the change to ABAC, there was a steady depression of the DO from March through May of 2021. Figure 18 shows all NOB and AOB K_O results determined from the declining DO test using VIP biomass, along with respective average DO concentrations within the full-scale VIP aeration basin.

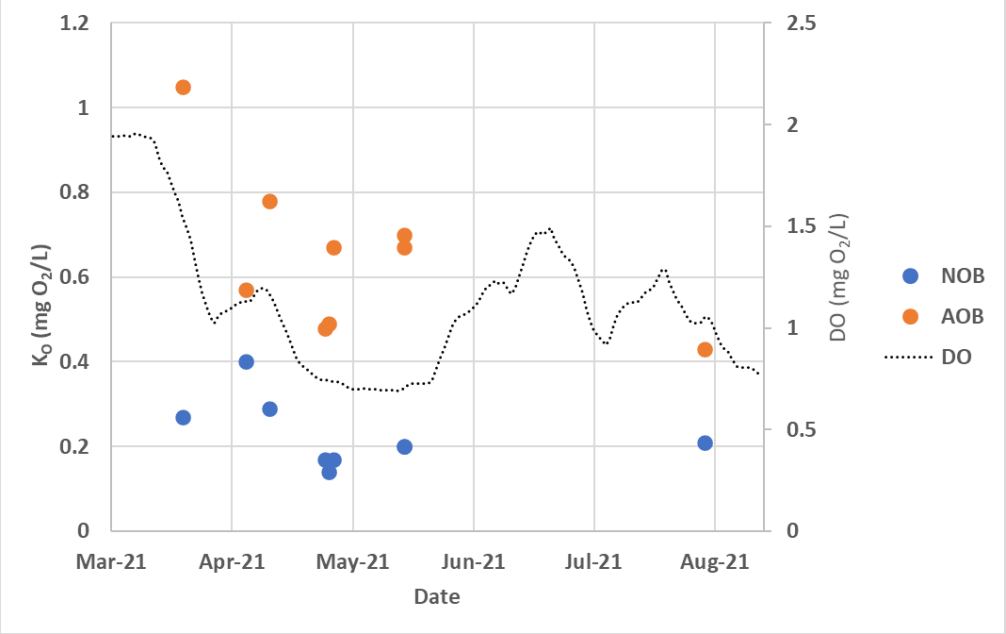

Figure 18. Oxygen half-saturation results for all declining DO tests conducted using VIP biomass samples over time, plotted with average DO within aeration zone.

In contrast to the K_O results measured in the parallel tests in Figure 16, there was an observed decrease in K_O as average DO decreased for both NOB and AOB in VIP biomass over time. Assuming floc morphology characteristics remained largely the same within the VIP full-scale facility, this suggested possible adaptation to decreasing DO conditions may have occurred for

nitrifiers over this period. To explore this relationship further, the K_O results from the declining DO test were plotted versus the average DO in the full-scale facility over a 30-day period prior to sample collection as shown in figure 19.

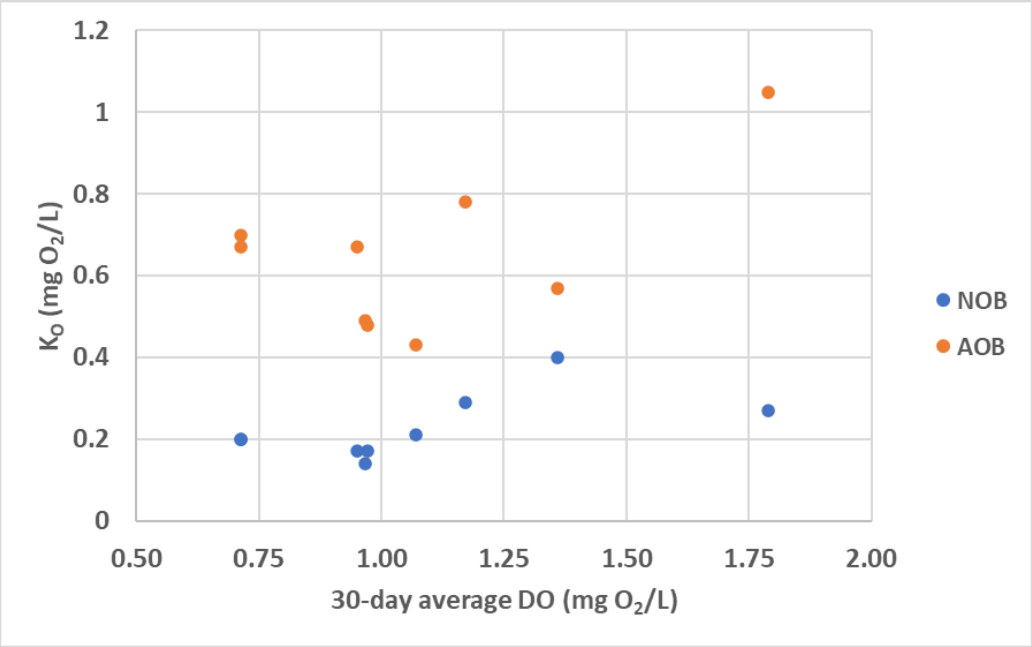

Figure 19. Oxygen half-saturation results for all declining DO tests conducted using VIP biomass vs. the 30-day average DO at time of sample collection.

Like the results found in the parallel test analysis, average DO concentrations in VIP's aeration basin facility were generally greater than the observed K_O values for both NOB and AOB. For that reason, adaptation pressures were likely not significant. However, assuming average floc sizes were comparable between all tests using VIP biomass, minor levels of adaptation for nitrifiers could have occurred as average DO concentrations decreased within the full-scale facility.

5. Conclusion

This study demonstrated the ability of the proposed declining DO method to distinctly measure the oxygen half-saturation values for NOB and AOB within a batch test reactor. Batch tests were conducted using a DO probe with a very fast response time and high data collection frequency. Experimental OUR data was measured and fit using a forward model. The forward model created a system of Monod equations which represented the oxygen kinetics for each functional group present within the test: endogenous respiration, NOB, and AOB. The system of equations was fit across the entire data set simultaneously by determining optimum parameter values (maximum oxygen uptake rate and oxygen half-saturation) for each functional group. An inverse model using Markov chain Monte Carlo analysis was applied to the results found in the forward model to provide statistical validation of the declining DO

method. Unlike versions of this method in existing literature, the use of selective inhibitors was avoided to maintain consistent biomass characteristics relative to full scale WWTPs.

The substrate utilization rate method was conducted in parallel with the declining DO method to verify oxygen half-saturation results. Biomass samples from three different full-scale HRSD treatment facilities (two BNR activated sludge and one MBR) were tested using the two methods. Parallel tests conducted using VIP biomass yielded a range of K_O values for both NOB and AOB. The range established using the declining DO method ($K_{O,NOB}$ = 0.21 – 0.30, $K_{O,AOB}$ = 0.43 – 0.85) was within the range determined using the substrate utilization rate method ($K_{O,NOB}$ = 0.09 – 0.34, $K_{O,AOB}$ = 0.28 – 1.15). For KWTP biomass, the observed K_O values for NOB and AOB were low, which proved more difficult to establish best fit curves through the substrate utilization rate test analysis. In the case of ABTP biomass, a significantly higher $K_{O,AOB}$ value was observed from the substrate utilization rate test relative to the declining DO test. This was assumed to be due to some experimental error associated with one or more of the substrate uptake rates used to fit a Monod curve and estimate K_O. The declining DO method provided nitrifier oxygen half-saturation estimates within ranges establishing by the substrate utilization rate method, while also appearing to be better suited for varying activated sludge samples and more resistant to potential experimental error.

Operating conditions for the WWTPs varied greatly, considering averages for DO, SRT, and floc size. Average floc size was found to have a strong correlation with the measured oxygen half-saturation values: as average floc size decreased, lower K_O values for both NOB and AOB were observed. When comparing the 30-day average DO concentration and SRT with measured K_O values, neither comparison yielded strong correlations. Measured K_O values for both NOB and AOB were lower than average DO concentrations at each full-scale facility, therefore there was likely little pressure for adaptation to occur. The comparison of results between VIP, ABTP, and KWTP facilities suggested that average floc size has the greatest effect on observed K_O values for nitrifiers observed within this study. Even though the average operating DO at KWTP was much higher than those at VIP and ABTP, the observed K_O values for nitrifiers was much lower. This could be due to a reduction in oxygen mass transfer limitations associated with larger floc sizes, a theory that has been supported in literature. Therefore, when comparing observed oxygen half-saturation values between treatment facilities, average floc size should also be considered. Results for all declining DO tests performed using VIP biomass were compiled, focusing on how changing operating conditions over time within the same full-scale facility could affect observed K_O values. Oxygen half-saturation values ranged from 0.14-0.40 mg O_2/L for $K_{O,NOB}$ and 0.43-1.05 mg O_2/L for $K_{O,AOB}$. In all cases, $K_{O,NOB} < K_{O,AOB}$, suggesting NOB were better suited to perform at low DO conditions compared to AOB.

Observed K_O results between the declining DO and substrate utilization rate methods within this study remained largely consistent for both NOB and AOB. Observed trends persisted between the two testing methods, and the declining DO method appeared to be more resistant to potential experimental error when compared to the substrate utilization rate method. The declining DO method can be conducted in half the time compared to that of the substrate utilization rate method and requires significantly less labor as well. The development of the

declining DO method without the use of selective inhibitors provided a more time and labor efficient technique for estimating apparent K_O values for NOB and AOB without sacrificing biomass integrity. Samples collected from variable full-scale operating conditions yielded consistent results between the two methods, providing further evidence that the proposed declining DO method can be a robust and reliable technique for distinctly measuring apparent K_O values for NOB and AOB.

References

Bertanza, G., Baroni, P., Garzetti, S., & Martinelli, F. (2021). Reducing energy demand by the combined application of Advanced Control Strategies in a full scale WWTP. *Water Science and Technology*, *83*(8), 1813–1823.

Blackburne, R., Vadivelu, V. M., Yuan, Z., & Keller, J. (2007). Determination of growth rate and yield of nitrifying bacteria by measuring carbon dioxide uptake rate. *Water Environment Research*, *79*(12), 2437–2445.

Brooks, S. P., & Gelman, A. (1998). General methods for monitoring convergence of iterative simulations. *Journal of Computational and Graphical Statistics*, *7*(4), 434.

Burton, F. L., Stensel, H. D., Tchobanoglous, G., & Metcalf & Eddy. (2003). *Wastewater engineering: Treatment and Reuse*. McGraw-Hill.

Chandran, K., & Smets, B. F. (2005). Optimizing experimental design to estimate ammonia and nitrite oxidation biokinetic parameters from batch respirograms. *Water Research*, *39*(20), 4969–4978.

Daigger, G. T., Adams, C. D., & Steller, H. K. (2007). Diffusion of oxygen through activated sludge flocs: Experimental measurement, modeling, and implications for simultaneous nitrification and Denitrification. *Water Environment Research*, *79*(4), 375–387.

Daebel, H., Manser, R., & Gujer, W. (2007). Exploring temporal variations of oxygen saturation constants of nitrifying bacteria. *Water Research*, *41*(5), 1094–1102.

De Mulder, C. *Impact of Intrinsic and Extrinsic Parameters on the Oxygen Kinetic Parameters of Ammonia and Nitrite Oxidizing Bacteria.* Master's Thesis, University of Gent. 2014

Environmental Protection Agency. Ammonia. (2021). *Causal Analysis/Diagnosis Decision Information System (CADDIS v.2)*. https://www.epa.gov/caddis-vol2/ammonia

Fan, H., Qi, L., Liu, G., Zhang, Y., Fan, Q., & Wang, H. (2016). Aeration optimization through operation at low dissolved oxygen concentrations: Evaluation of oxygen mass transfer dynamics in different activated sludge systems. *Journal of Environmental Sciences*, *55*, 224–235.

Fang, F., Ni, B.-J., Li, X.-Y., Sheng, G.-P., & Yu, H.-Q. (2009). Kinetic analysis on the two-step processes of AOB and NOB in aerobic nitrifying granules. *Applied Microbiology and Biotechnology*, *83*(6), 1159–1169.

Gelman, A., Gilks, W. R., & Roberts, G. O. (1997). Weak convergence and optimal scaling of Random Walk Metropolis algorithms. *The Annals of Applied Probability*, *7*(1).

Ghimire, B.K. *Investigation of oxygen half saturation coefficients for nitrification.* Master's Thesis, Tribhuvan University, Nepal. 2000.

Grady Jr, C.L., Daigger, G.T., Love, N.G., Filipe, C.D., Leslie Grady, C., 2011. *Biological Wastewater Treatment*: IWA Publishing.

Guisasola, A., Jubany, I., Baeza, J. A., Carrera, J., & Lafuente, J. (2005). Respirometric estimation of the oxygen affinity constants for biological ammonium and nitrite oxidation. *Journal of Chemical Technology & Biotechnology*, *80*(4), 388–396.

Jones, R. M., Dold, P. L., Takács, I., Chapman, K., Wett, B., Murthy, S., & Shaughnessy, M. O. (2007). Simulation for operation and control of reject water treatment processes. *Proceedings of the Water Environment Federation*, *2007*(14), 4357–4372.

Jubany, I., Baeza, J. A., Carrera, J., & Lafuente, J. (2005). Respirometric calibration and validation of a biological nitrite oxidation model including biomass growth and substrate inhibition. *Water Research*, *39*(18), 4574–4584.

Keene, N. A., Reusser, S. R., Scarborough, M. J., Grooms, A. L., Seib, M., Santo Domingo, J., & Noguera, D. R. (2017). Pilot plant demonstration of stable and efficient high rate biological nutrient removal with low dissolved oxygen conditions. *Water Research*, *121*, 72–85.

Liu, G., & Wang, J. (2012). Probing the stoichiometry of the nitrification process using the respirometric approach. *Water Research*, *46*(18), 5954–5962.

Liu, G., & Wang, J. (2015). Modeling effects of do and SRT on activated sludge decay and production. *Water Research*, *80*, 169–178.

Manser, R., Gujer, W., & Siegrist, H. (2005). Consequences of mass transfer effects on the kinetics of nitrifiers. *Water Research*, *39*(19), 4633–4642.

Ordaz, A., Oliveira, C. S., Aguilar, R., Carrión, M., Ferreira, E. C., Alves, M., & Thalasso, F. (2008). Kinetic and stoichiometric parameters estimation in a nitrifying bubble column through "in-situ" pulse respirometry. *Biotechnology and Bioengineering*, *100*(1), 94–102.

Pai, T.-Y., Wan, T.-J., Tsai, Y.-P., Tzeng, C.-J., Chu, H.-H., Tsai, Y.-S., & Lin, C.-Y. (2010). Effect of sludge retention time on nitrifiers' biomass and kinetics in an anaerobic/oxic process. *CLEAN - Soil, Air, Water*, *38*(2), 167–172.

Picioreanu, C., Pérez, J., & van Loosdrecht, M. C. M. (2016). Impact of cell cluster size on apparent half-saturation coefficients for oxygen in nitrifying sludge and biofilms. *Water Research*, *106*, 371–382.

Raftery, A., & Lewis, S. (1995). The Number of Iterations, Convergence Diagnostics and Generic Metropolis Algorithms. *Practical Markov Chain Monte Carlo*.

Sanchez, O., Marti, M. C., Aspe, E., & Roeckel, M. (2001). Nitrification rates in a saline medium at different dissolved oxygen concentrations. *Biotechnology Letters,* 23, 1597-1602

Shaw, A., *Investigating the Significance of Half-Saturation Coefficients on Wastewater Treatment Processes.* PhD Dissertation, Illinois Institute of Technology. 2015.

Soetaert, K., & Petzoldt, T. (2010). Inverse modelling, sensitivity and Monte Carlo Analysis in R Using Package FME. *Journal of Statistical Software*, *33*(3).

Torretta, V., Ragazzi, M., Trulli, E., De Feo, G., Urbini, G., Raboni, M., & Rada, E. (2014). Assessment of Biological Kinetics in a conventional municipal wwtp by means of the oxygen uptake rate method. *Sustainability*, *6*(4), 1833–1847.

Val del Rio, A., Campos, J. L., Da Silva, C., Pedrouso, A., & Mosquera-Corral, A. (2019). Determination of the intrinsic kinetic parameters of ammonia-oxidizing and nitrite-oxidizing bacteria in granular and flocculent sludge. *Separation and Purification Technology*, *213*, 571–577.

van de Schoot, R., Depaoli, S., King, R., Kramer, B., Märtens, K., Tadesse, M. G., Vannucci, M., Gelman, A., Veen, D., Willemsen, J., & Yau, C. (2021). Bayesian statistics and modelling. *Nature Reviews Methods Primers*, *1*(1).

van Loosdrecht, M. C. M., Nielson, P. H., Lopez-Vasquez, C. M., & Brdjanovic, D. (2016). *Experimental methods in wastewater treatment*. IWA Publishing.

Appendix A. Supplementary Material

Parallel Test Results

VIP 4-23-2021

Table 13. (4-23-2021 VIP) parallel test mean and standard deviation value results from combined MCMC inverse model

Parameter	Mean	Standard Deviation
OUR_{END}^{max}	6.13 mg O_2/L/hr	0.069
$K_{O,END}$	0.23 mg O_2/L	0.008
OUR_{NOB}^{max}	2.46 mg O_2/L/hr	0.091
$K_{O,NOB}$	0.40 mg O_2/L	0.038
OUR_{AOB}^{max}	6.46 mg O_2/L/hr	0.120
$K_{O,AOB}$	0.57 mg O_2/L	0.032

Table 14. (4-23-2021 VIP) Parallel test quantile results from combined MCMC inverse model

Parameter	2.5%	25%	50%	75%	97.5%
OUR_{END}^{max}	5.99	6.08	6.13	6.17	6.26
$K_{O,END}$	0.22	0.23	0.23	0.24	0.25
OUR_{NOB}^{max}	2.28	2.40	2.46	2.52	2.64
$K_{O,NOB}$	0.33	0.37	0.40	0.43	0.48
OUR_{AOB}^{max}	6.23	6.38	6.46	6.54	6.70
$K_{O,AOB}$	0.51	0.54	0.57	0.59	0.63

Table 15. (4-23-2021 VIP) parallel test summary of substrate utilization rates for NOB and AOB

DO Setpoint (mg O_2/L)	NUR (mg NO_2^-/L/hr)	AUR (mg NH_3/L/hr)
0.1	1.31	0.09
0.21	2.82	1.97
0.48	3.92	4.08
1.0	6.12	6.06
2.0	4.56	4.75
3.0	3.96	3.66
6.0	5.04	4.70

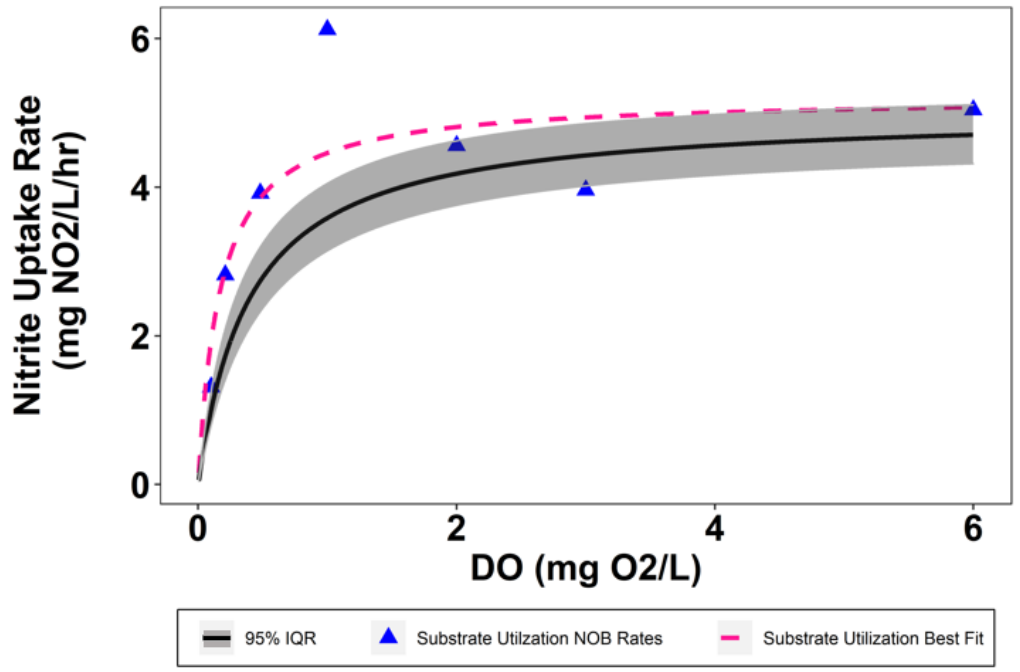

Figure 20. (4-23-2021 VIP) NUR vs. DO results comparison between declining DO and substrate utilization rate batch tests.

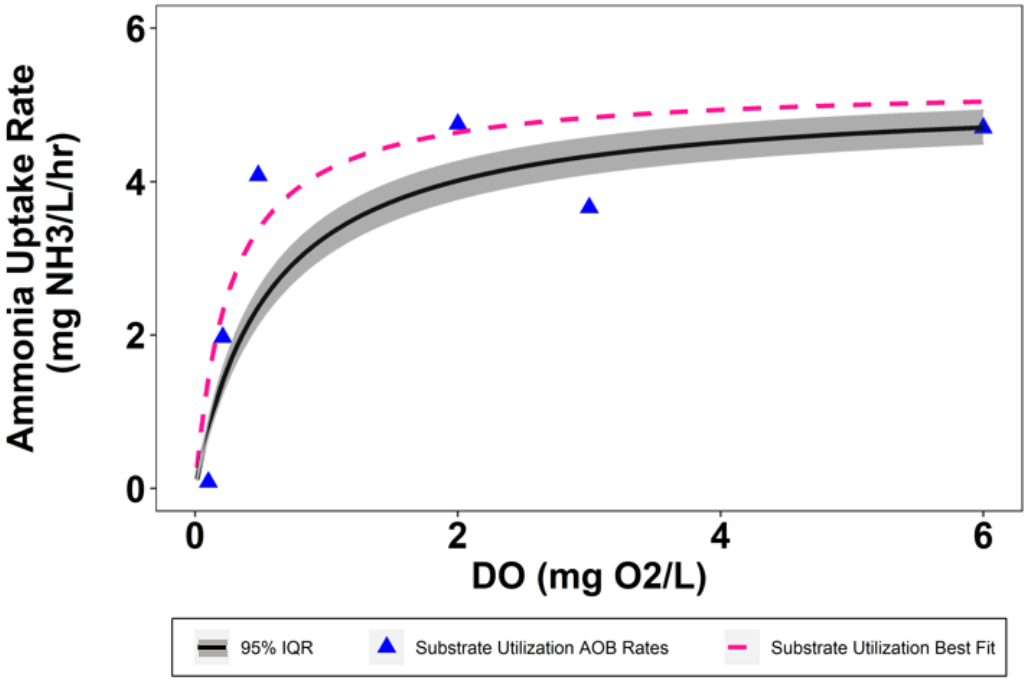

Figure 21. (4-23-2021 VIP) AUR vs. DO results comparison between declining DO and substrate utilization rate batch tests.

VIP 4-29-2021

Table 16. (4-29-2021 VIP) Parallel test mean and standard deviation value results from combined MCMC inverse model

Parameter	Mean	Standard Deviation
OUR_{END}^{max}	8.73 mg O_2/L/hr	0.055
$K_{O,END}$	0.12 mg O_2/L	0.002
OUR_{NOB}^{max}	1.21 mg O_2/L/hr	0.066
$K_{O,NOB}$	0.30 mg O_2/L	0.042
OUR_{AOB}^{max}	9.30 mg O_2/L/hr	0.101
$K_{O,AOB}$	0.78 mg O_2/L	0.028

Table 17. (4-29-2021 VIP) Parallel test quantile results from combined MCMC inverse model

Parameter	2.5%	25%	50%	75%	97.5%
OUR_{END}^{max}	8.62	8.70	8.73	8.77	8.84
$K_{O,END}$	0.11	0.12	0.12	0.12	0.12
OUR_{NOB}^{max}	1.08	1.16	1.21	1.25	1.34
$K_{O,NOB}$	0.22	0.27	0.29	0.32	0.39
OUR_{AOB}^{max}	9.09	9.23	9.30	9.37	9.51
$K_{O,AOB}$	0.73	0.76	0.78	0.80	0.84

Table 18. (4-29-2021 VIP) Parallel test summary of substrate utilization rates for NOB and AOB

DO Setpoint (mg O_2/L)	NUR (mg NO_2^-/L/hr)	AUR (mg NH_3/L/hr)
0.09	1.19	0.07
0.22	2.54	0.32
0.6	4.90	3.60
1.0	4.11	3.46
2.0	6.09	5.94
3.0	6.51	6.55
6.0	5.93	6.29

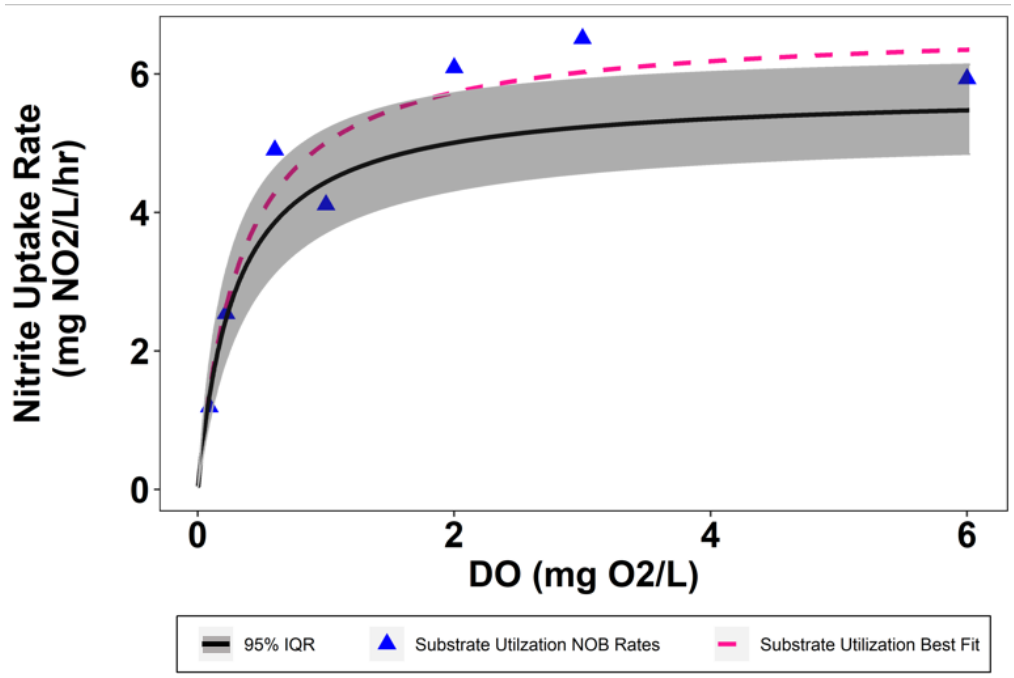

Figure 22. (4-29-2021 VIP) NUR vs. DO results comparison between declining DO and substrate utilization rate batch tests.

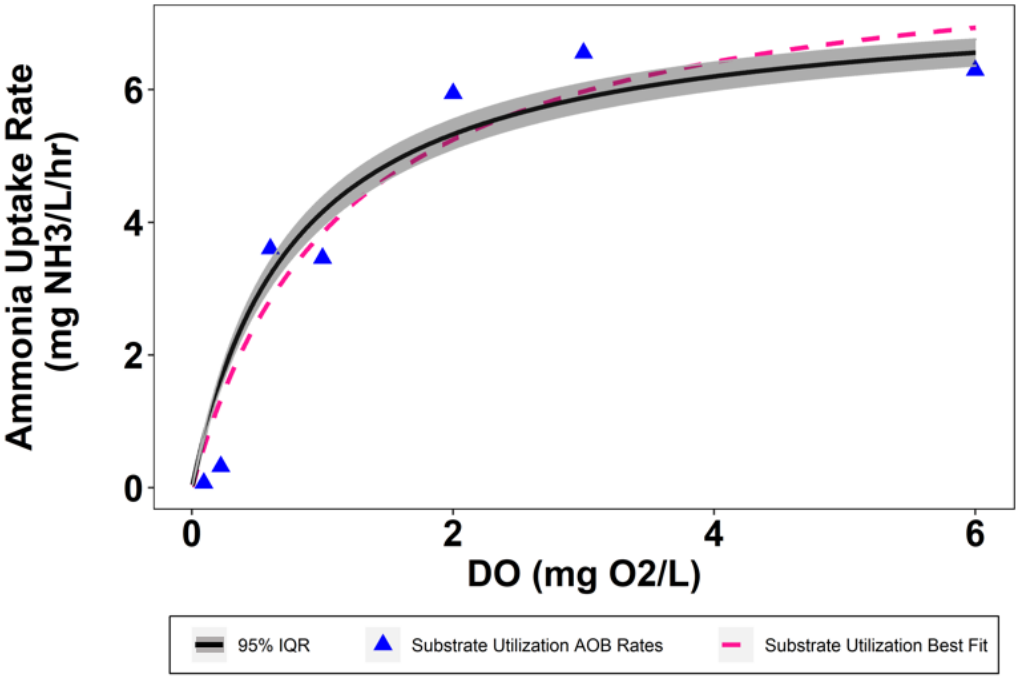

Figure 23. (4-29-2021 VIP) AUR vs. DO results comparison between declining DO and substrate utilization rate batch tests.

King William Treatment Plant 5-18-2021

Table 19. (5-18-2021 KWTP) Parallel test mean and standard deviation value results from combined MCMC inverse model

Parameter	Mean	Standard Deviation
OUR_{END}^{max}	11.22 mg O_2/L/hr	0.108
$K_{O,END}$	0.06 mg O_2/L	0.002
OUR_{NOB}^{max}	4.20 mg O_2/L/hr	0.116
$K_{O,NOB}$	0.07 mg O_2/L	0.007
OUR_{AOB}^{max}	24.01 mg O_2/L/hr	0.103
$K_{O,AOB}$	0.09 mg O_2/L	0.003

Table 20. (5-18-2021 KWTP) Parallel test quantile results from combined MCMC inverse model

Parameter	2.5%	25%	50%	75%	97.5%
OUR_{END}^{max}	11.00	11.14	11.22	11.29	11.42
$K_{O,END}$	0.05	0.06	0.06	0.06	0.06
OUR_{NOB}^{max}	3.97	4.12	4.19	4.27	4.43
$K_{O,NOB}$	0.06	0.07	0.07	0.08	0.09
OUR_{AOB}^{max}	23.80	23.94	24.01	24.08	24.21
$K_{O,AOB}$	0.09	0.09	0.09	0.10	0.10

Table 21. (5-18-2021 KWTP) Parallel test summary of substrate utilization rates for NOB and AOB

DO Setpoint (mg O_2/L)	NUR (mg NO_2^-/L/hr)	AUR (mg NH_3/L/hr)
0.12	7.59	6.47
0.26	7.18	5.65
0.66	7.94	7.11
1.0	7.44	6.97
2.0	6.34	5.86
3.0	6.34	6.37
6.0	8.05	7.98

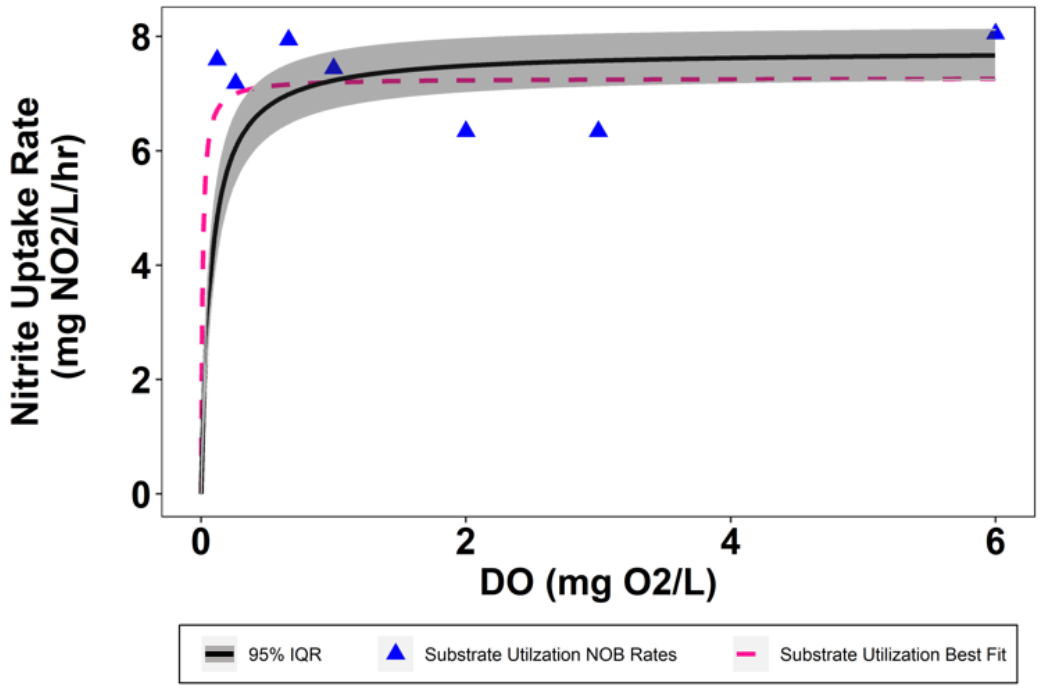

Figure 24. (5-18-2021 KWTP) NUR vs. DO results comparison between declining DO and substrate utilization rate batch tests.

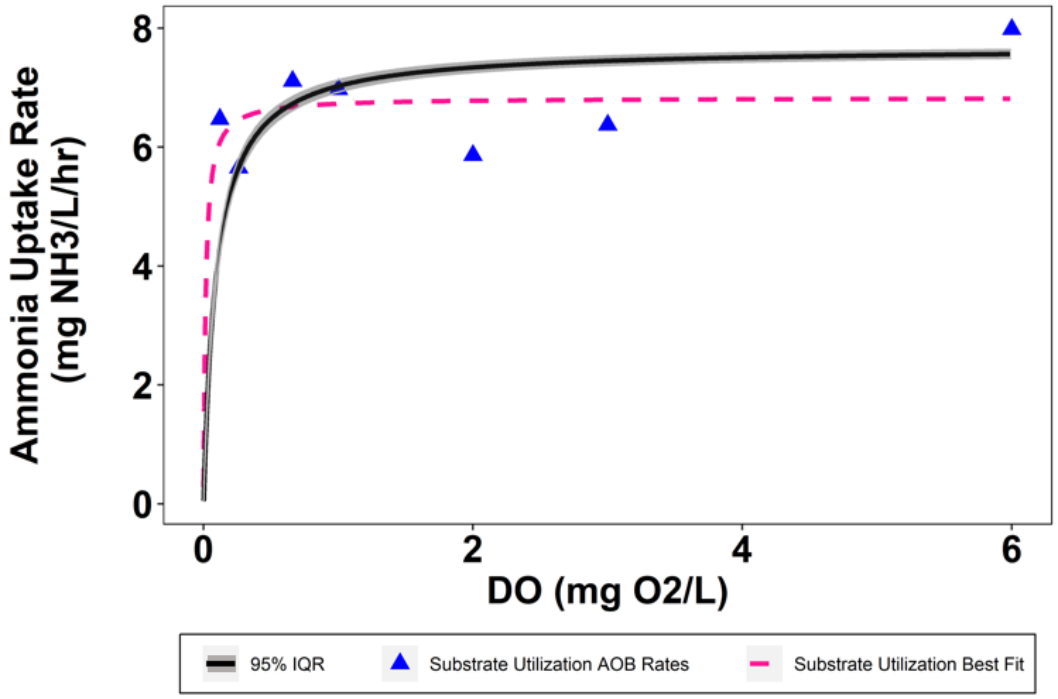

Figure 25. (5-18-2021 KWTP) AUR vs. DO results comparison between declining DO and substrate utilization rate batch tests.

ABTP 5-27-2021

Table 22. (5-27-2021 ABTP) Parallel test mean and standard deviation value results from combined MCMC inverse model

Parameter	Mean	Standard Deviation
OUR_{END}^{max}	5.21 mg O_2/L/hr	0.130
$K_{O,END}$	0.16 mg O_2/L	0.016
OUR_{NOB}^{max}	10.31 mg O_2/L/hr	0.174
$K_{O,NOB}$	0.43 mg O_2/L	0.025
OUR_{AOB}^{max}	15.65 mg O_2/L/hr	0.194
$K_{O,AOB}$	0.70 mg O_2/L	0.032

Table 23. (5-27-2021 ABTP) Parallel test quantile results from combined MCMC inverse model

Parameter	2.5%	25%	50%	75%	97.5%
OUR_{END}^{max}	4.96	5.12	5.21	5.30	5.47
$K_{O,END}$	0.13	0.15	0.16	0.17	0.19
OUR_{NOB}^{max}	9.97	10.18	10.31	10.43	10.65
$K_{O,NOB}$	0.38	0.41	0.42	0.44	0.48
OUR_{AOB}^{max}	15.28	15.52	15.65	15.78	16.05
$K_{O,AOB}$	0.64	0.67	0.70	0.72	0.76

Table 24. (5-27-2021 ABTP) Parallel test summary of substrate utilization rates for NOB and AOB

DO Setpoint (mg O_2/L)	NUR (mg NO_2^-/L/hr)	AUR (mg NH_3/L/hr)
0.09	2.09	0.38
0.21	4.83	1.86
0.42	5.29	2.25
1.0	6.64	3.84
2.0	9.36	9.47
3.0	11.31	12.33
6.0	10.32	11.21

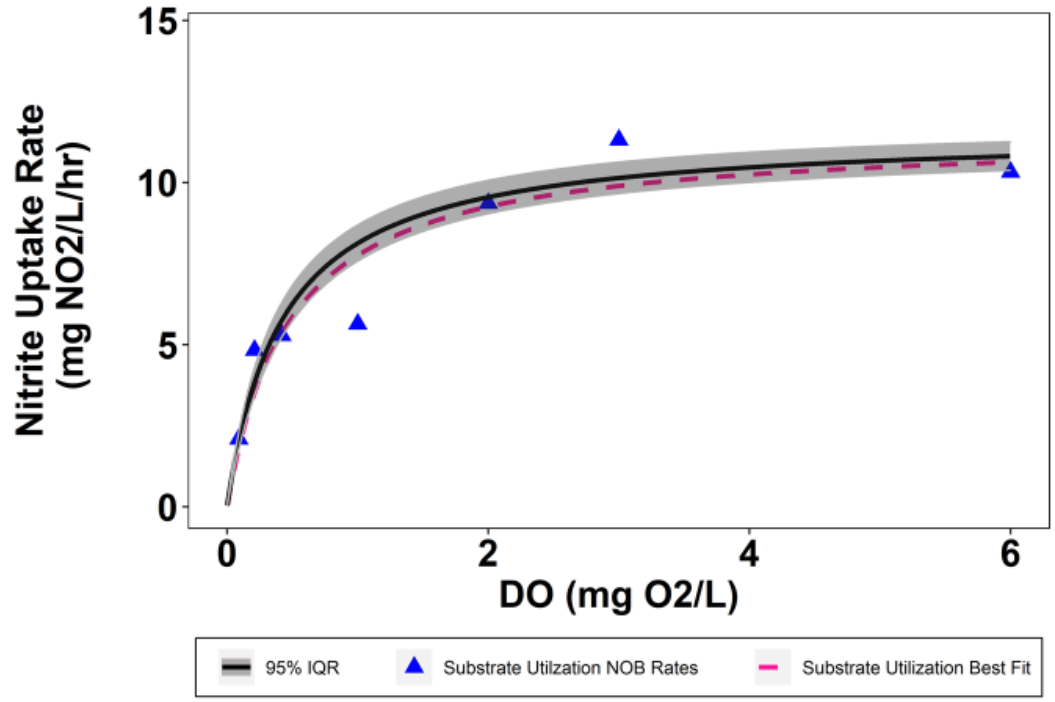

Figure 26. (5-27-2021 ABTP) NUR vs. DO results comparison between declining DO and substrate utilization rate batch tests.

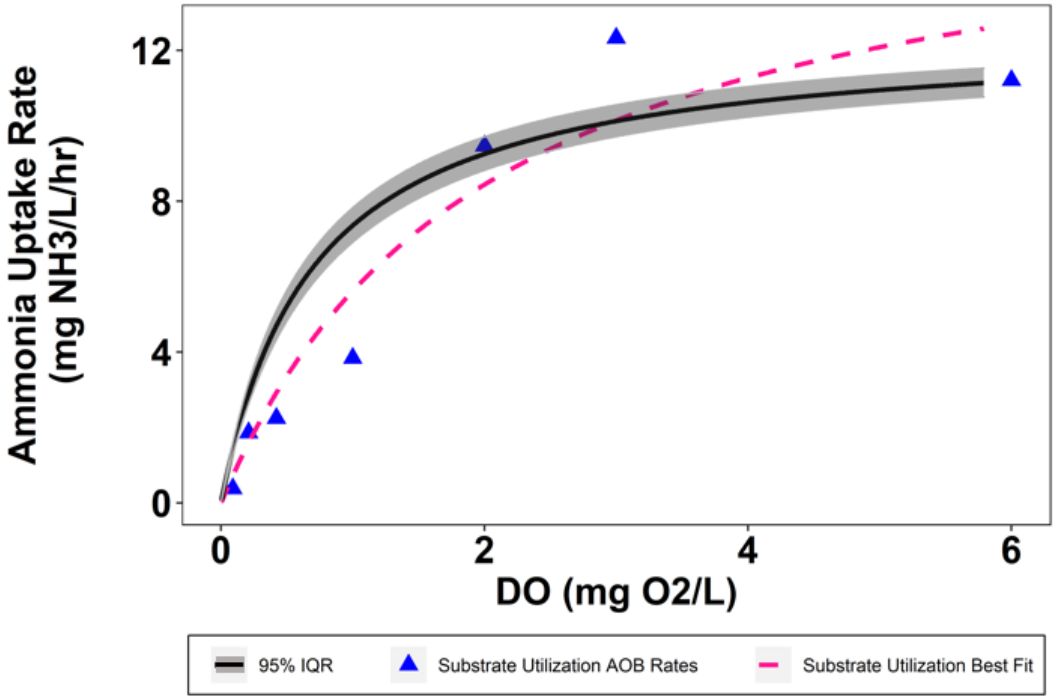

Figure 27. (5-27-2021 ABTP) AUR vs. DO results comparison between declining DO and substrate utilization rate batch tests.

VIP 8-17-2021

Table 25. (8-17-2021 VIP) Parallel test mean and standard deviation value results from combined MCMC inverse model

Parameter	Mean	Standard Deviation
OUR_{END}^{max}	3.89 mg O_2/L/hr	0.050
$K_{O,END}$	0.06 mg O_2/L	0.005
OUR_{NOB}^{max}	5.62 mg O_2/L/hr	0.066
$K_{O,NOB}$	0.22 mg O_2/L	0.013
OUR_{AOB}^{max}	9.66 mg O_2/L/hr	0.088
$K_{O,AOB}$	0.42 mg O_2/L	0.019

Table 26. (8-17-2021 VIP) Parallel test quantile results from combined MCMC inverse model

Parameter	2.5%	25%	50%	75%	97.5%
OUR_{END}^{max}	3.80	3.86	3.89	3.93	3.99
$K_{O,END}$	0.061	0.066	0.069	0.073	0.079
OUR_{NOB}^{max}	5.49	5.58	5.62	5.67	5.75
$K_{O,NOB}$	0.18	0.20	0.21	0.21	0.23
OUR_{AOB}^{max}	9.49	9.60	9.66	9.72	9.83
$K_{O,AOB}$	0.39	0.41	0.42	0.44	0.46

Table 27. (8-17-2021 VTP) Parallel test summary of substrate utilization rates for NOB and AOB

DO Setpoint (mg O_2/L)	NUR (mg NO_2^-/L/hr)	AUR (mg NH_3/L/hr)
0.07	2.21	0.09
0.22	4.63	1.42
0.55	5.76	2.82
1.0	6.06	3.61
2.0	5.52	3.56
3.0	6.72	4.54
6.0	5.28	3.51

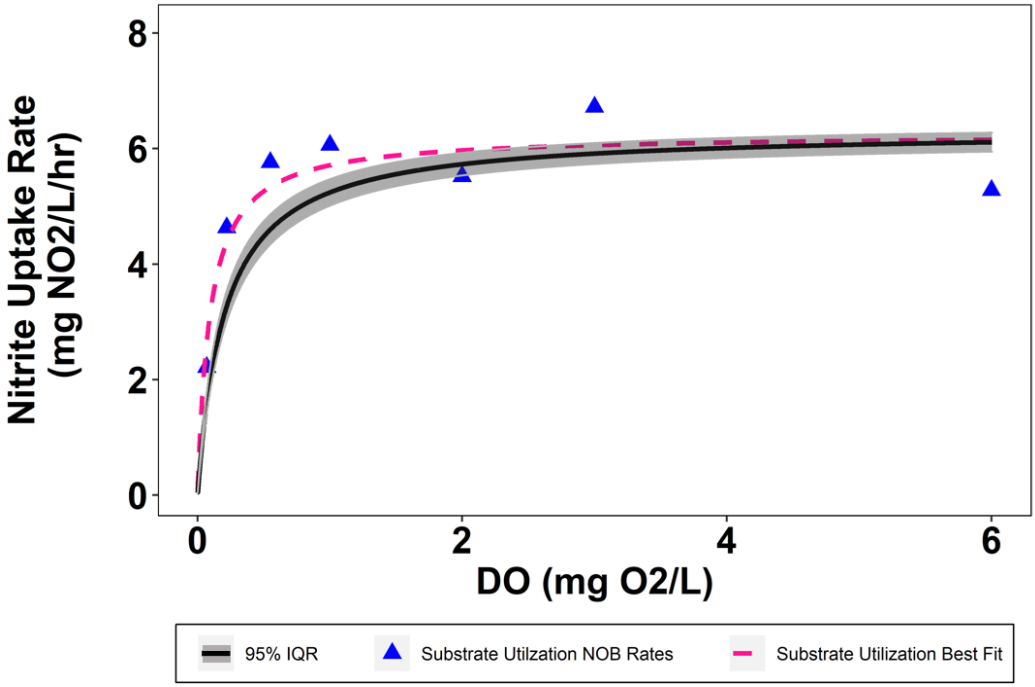

Figure 28. (8-17-2021 VIP) NUR vs. DO results comparison between declining DO and substrate utilization rate batch tests.

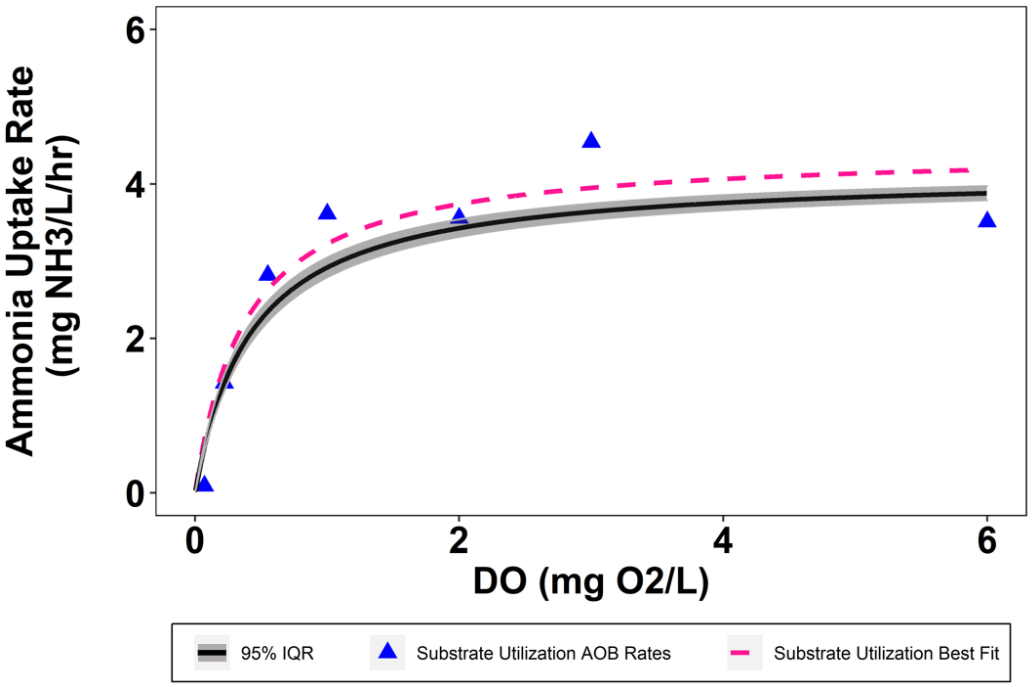

Figure 29. (8-17-2021 VIP) AUR vs. DO results comparison between declining DO and substrate utilization rate batch tests.

VIP Declining DO Test Results

4-7-2021

Table 28. (4-7-2021 VIP) Mean and standard deviation value results from combined MCMC inverse model

Parameter	Mean	Standard Deviation
OUR_{END}^{max}	5.76 mg O_2/L/hr	0.049
$K_{O,END}$	0.06 mg O_2/L	0.003
OUR_{NOB}^{max}	3.76 mg O_2/L/hr	0.070
$K_{O,NOB}$	0.27 mg O_2/L	0.020
OUR_{AOB}^{max}	16.90 mg O_2/L/hr	0.085
$K_{O,AOB}$	1.06 mg O_2/L	0.030

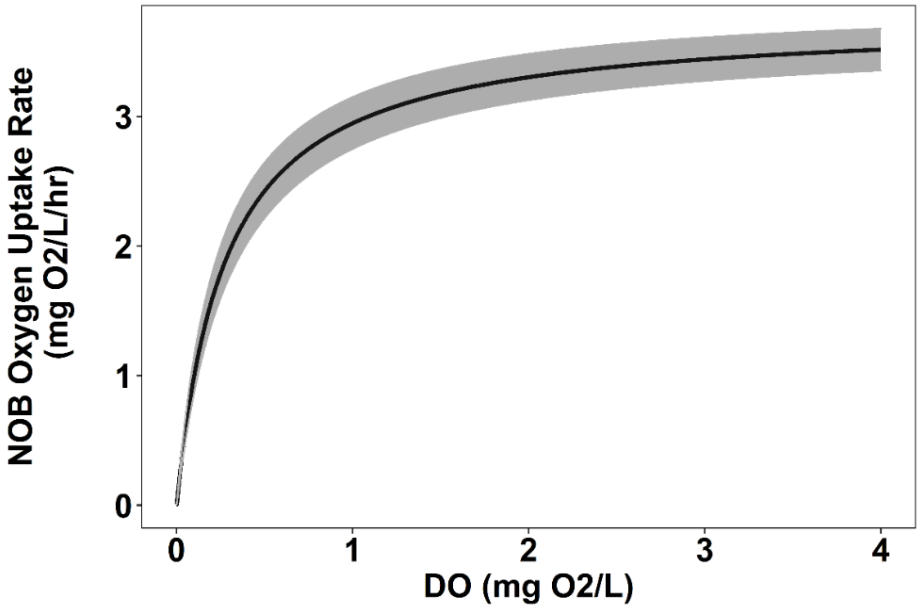

Figure 30. (4-7-2021 VIP) Final NOB OUR curve (with 95% IQR) from combined MCMC analysis.

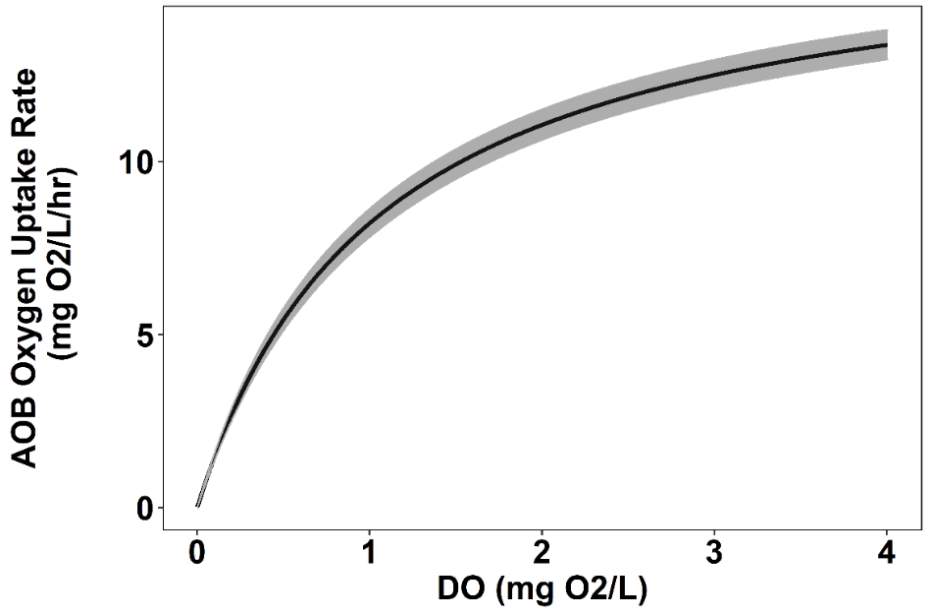

Figure 31. (4-7-2021 VIP) Final AOB OUR curve (with 95% IQR) from combined MCMC analysis.

5-13-2021

Table 29. (5-13-2021 VIP) Mean and standard deviation value results from combined MCMC inverse model

Parameter	Mean	Standard Deviation
OUR_{END}^{max}	3.34 mg O_2/L/hr	0.037
$K_{O,END}$	0.09 mg O_2/L	0.004
OUR_{NOB}^{max}	2.91 mg O_2/L/hr	0.045
$K_{O,NOB}$	0.17 mg O_2/L	0.010
OUR_{AOB}^{max}	10.81 mg O_2/L/hr	0.079
$K_{O,AOB}$	0.48 mg O_2/L	0.014

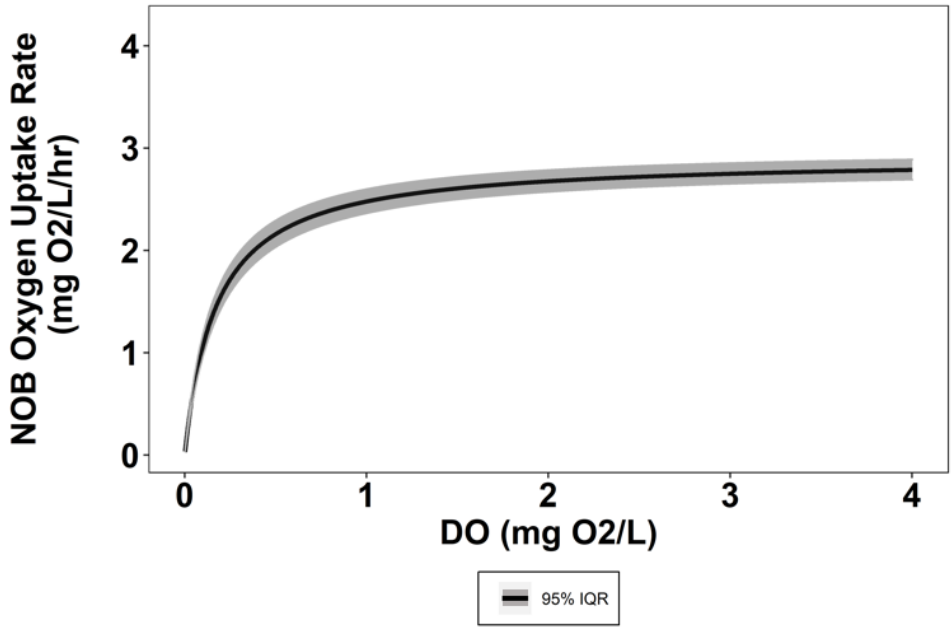

Figure 32. (5-13-2021 VIP) Final NOB OUR curve (with 95% IQR) from combined MCMC analysis.

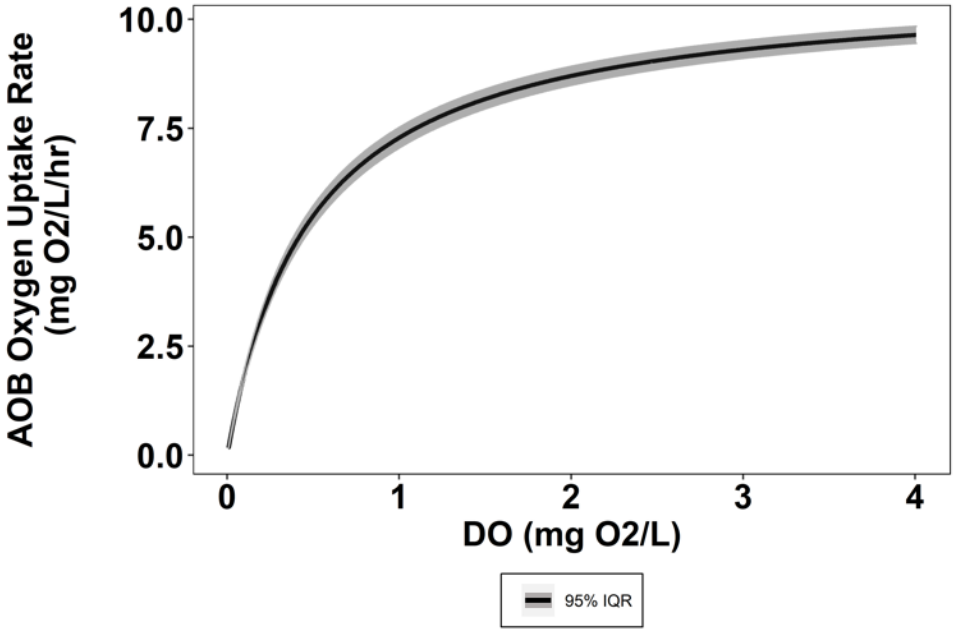

Figure 33. (5-13-2021 VIP) Final AOB OUR curve (with 95% IQR) from combined MCMC analysis.

5-14-2021

Table 30. (5-14-2021 VIP) Mean and standard deviation value results from combined MCMC inverse model

Parameter	Mean	Standard Deviation
OUR_{END}^{max}	4.36 mg O_2/L/hr	0.045
$K_{O,END}$	0.07 mg O_2/L	0.004
OUR_{NOB}^{max}	4.16 mg O_2/L/hr	0.057
$K_{O,NOB}$	0.14 mg O_2/L	0.009
OUR_{AOB}^{max}	13.07 mg O_2/L/hr	0102
$K_{O,AOB}$	0.49 mg O_2/L	0.015

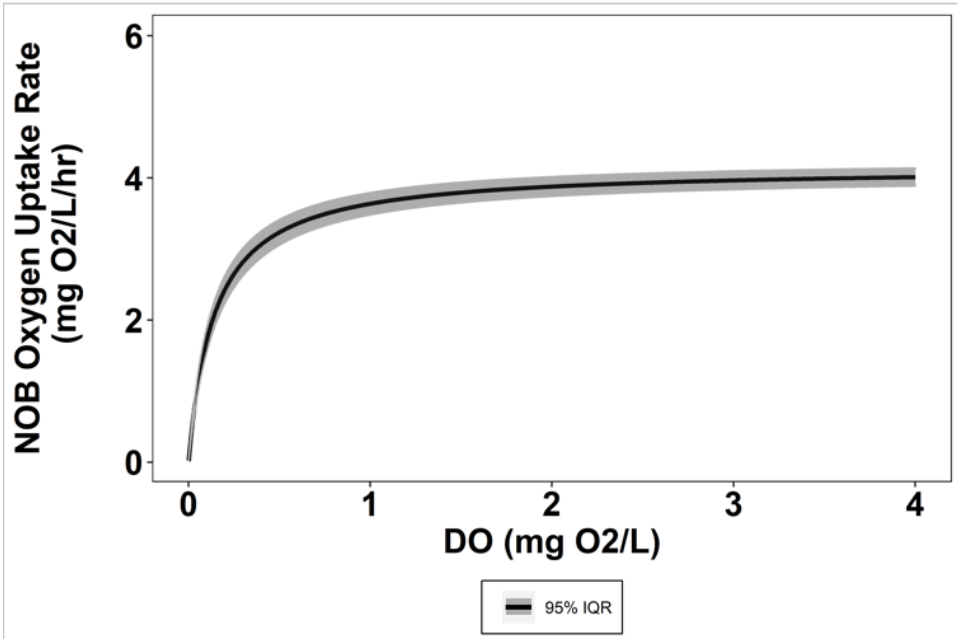

Figure 34. (5-14-2021 VIP) Final NOB OUR curve (with 95% IQR) from combined MCMC analysis.

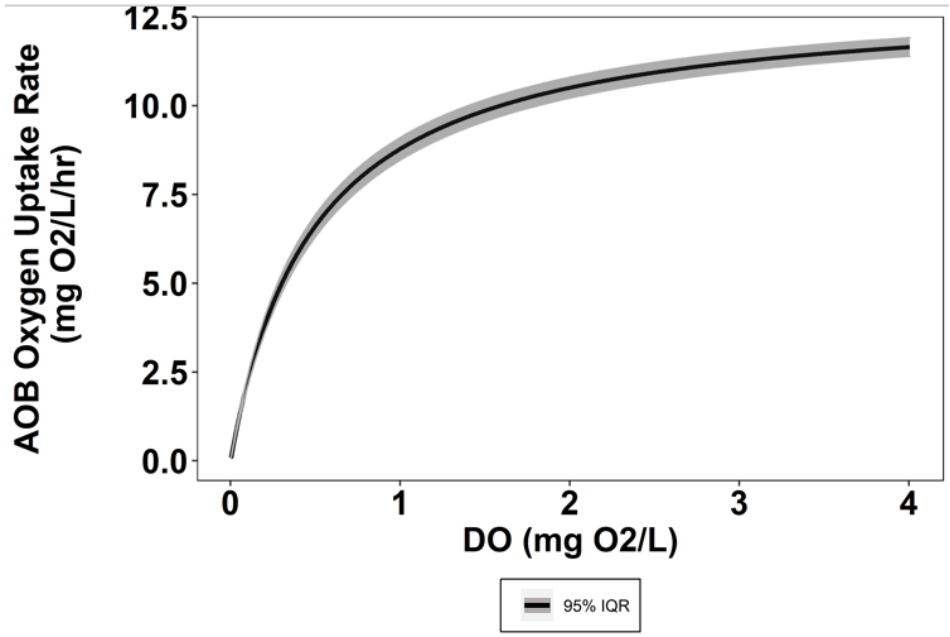

Figure 35. (5-14-2021 VIP) Final AOB OUR curve (with 95% IQR) from combined MCMC analysis.

5-15-2021

Table 31. (5-15-2021 VIP) Mean and standard deviation value results from combined MCMC inverse model

Parameter	Mean	Standard Deviation
OUR_{END}^{max}	4.17 mg O_2/L/hr	0.040
$K_{O,END}$	0.10 mg O_2/L	0.004
OUR_{NOB}^{max}	4.89 mg O_2/L/hr	0.052
$K_{O,NOB}$	0.17 mg O_2/L	0.007
OUR_{AOB}^{max}	17.06 mg O_2/L/hr	0.114
$K_{O,AOB}$	0.67 mg O_2/L	0.015

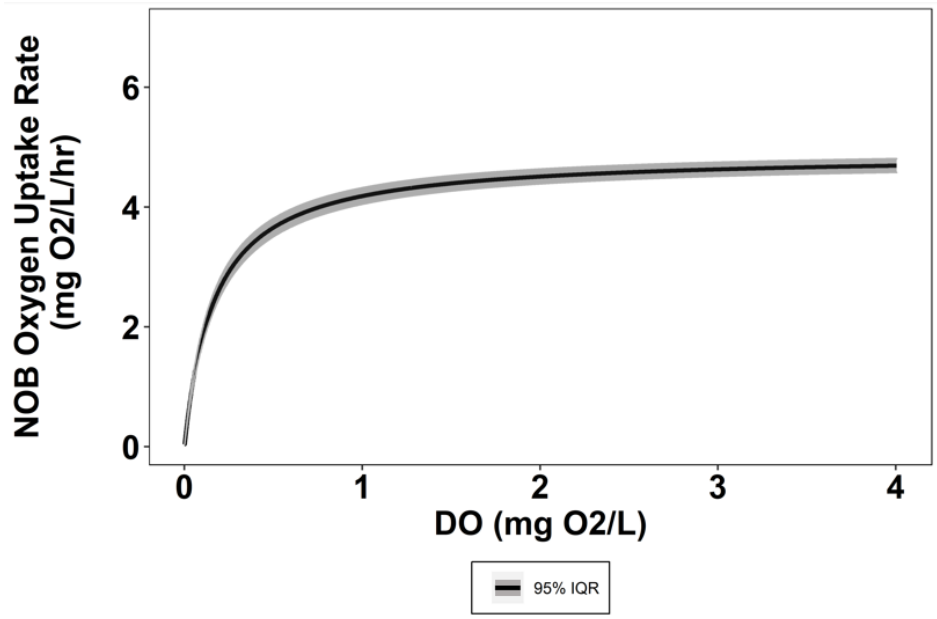

Figure 36. (5-15-2021 VIP) Final NOB OUR curve (with 95% IQR) from combined MCMC analysis.

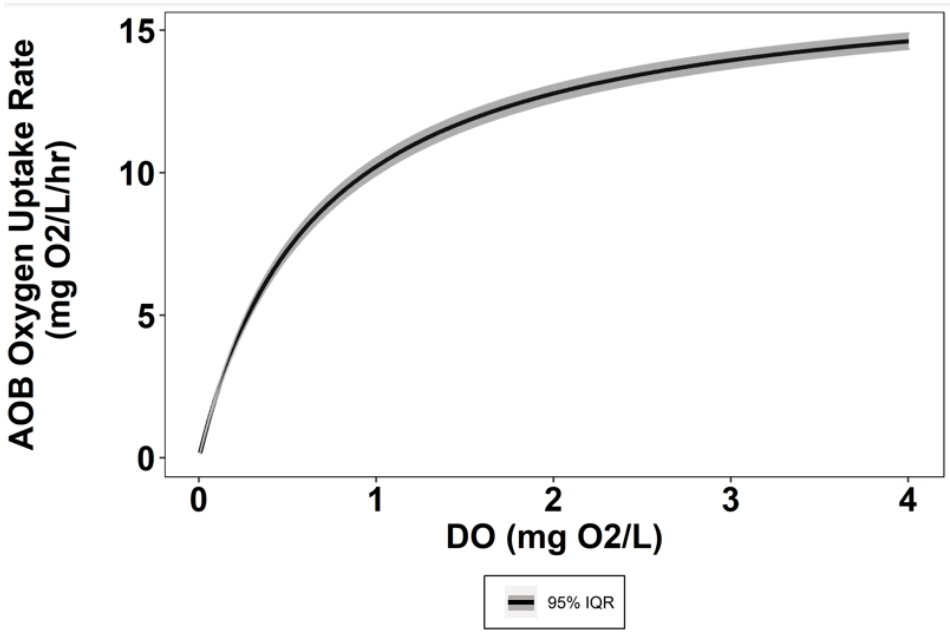

Figure 37. (5-15-2021 VIP) Final AOB OUR curve (with 95% IQR) from combined MCMC analysis.

6-2-2021 (Test #1)

Table 32. (6-2-2021 VIP Test #1) Mean and standard deviation value results from combined MCMC inverse model

Parameter	Mean	Standard Deviation
OUR_{END}^{max}	4.51 mg O_2/L/hr	0.038
$K_{O,END}$	0.07 mg O_2/L	0.003
OUR_{NOB}^{max}	5.12 mg O_2/L/hr	0.054
$K_{O,NOB}$	0.20 mg O_2/L	0.010
OUR_{AOB}^{max}	17.94 mg O_2/L/hr	0.110
$K_{O,AOB}$	0.67 mg O_2/L	0.014

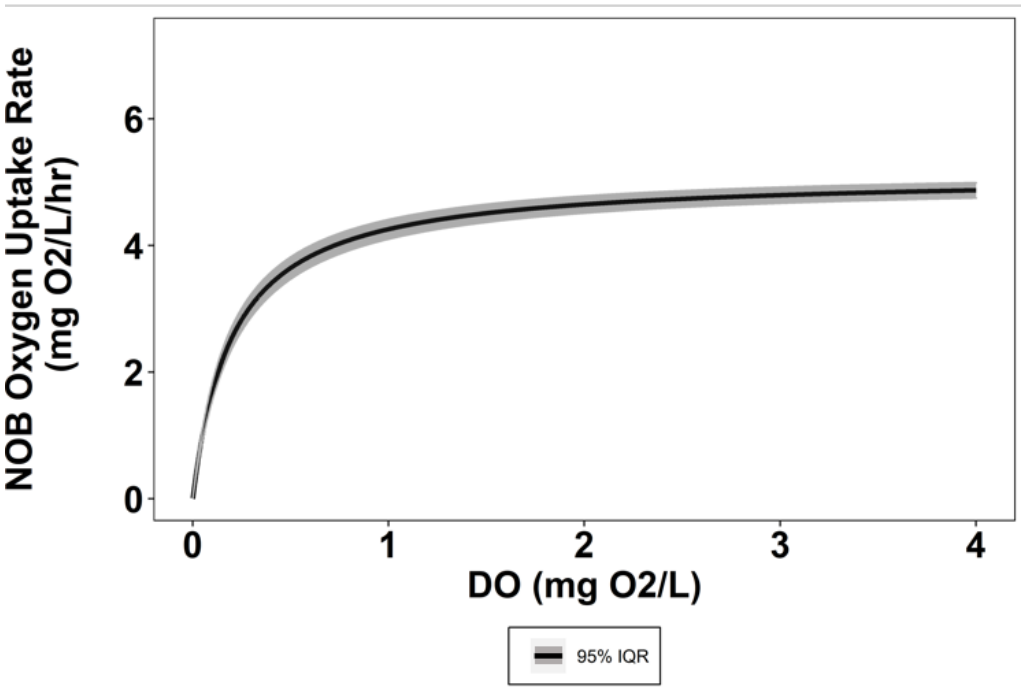

Figure 38. (6-2-2021 VIP Test #1) Final NOB OUR curve (with 95% IQR) from combined MCMC analysis.

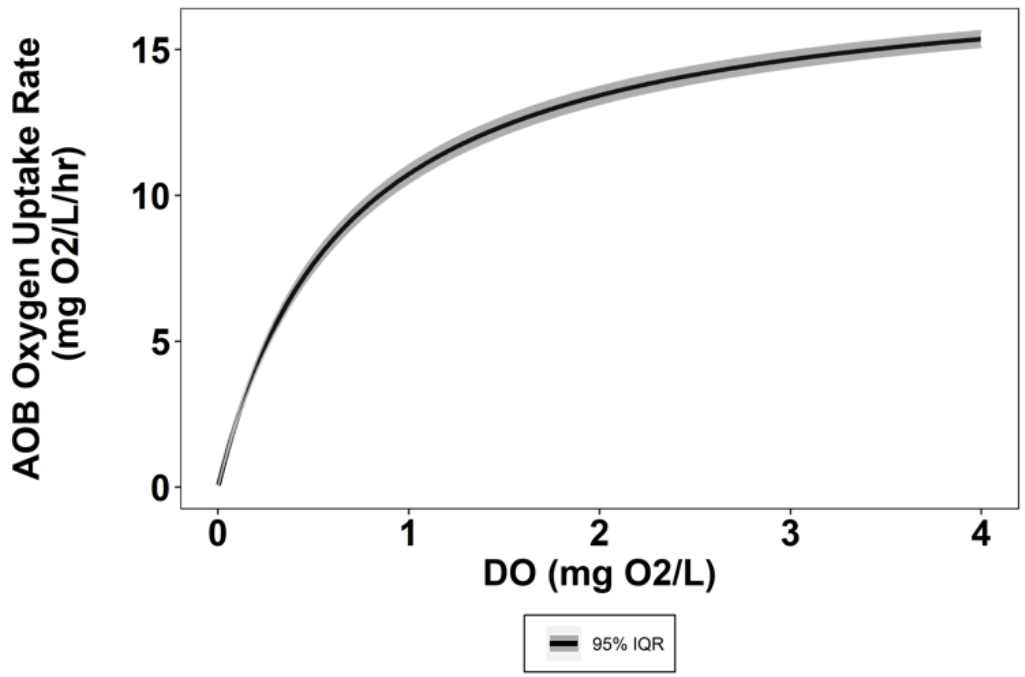

Figure 39. (6-2-2021 VIP Test #1) Final AOB OUR curve (with 95% IQR) from combined MCMC analysis.

6-2-2021 (Test #2)

Table 33. (6-2-2021 VIP Test #2) Mean and standard deviation value results from combined MCMC inverse model

Parameter	Mean	Standard Deviation
OUR_{END}^{max}	4.34 mg O_2/L/hr	0.037
$K_{O,END}$	0.7 mg O_2/L	0.003
OUR_{NOB}^{max}	4.14 mg O_2/L/hr	0.051
$K_{O,NOB}$	0.20 mg O_2/L	0.011
OUR_{AOB}^{max}	16.42 mg O_2/L/hr	0.107
$K_{O,AOB}$	0.70 mg O_2/L	0.015

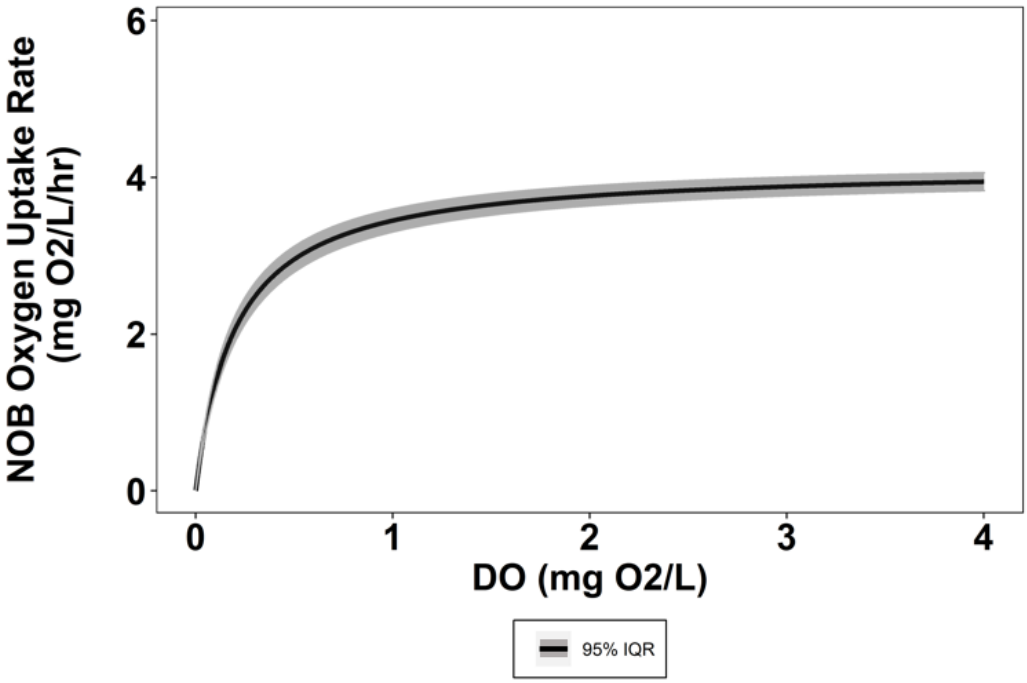

Figure 40. (6-2-2021 VIP Test #2) Final NOB OUR curve (with 95% IQR) from combined MCMC analysis.

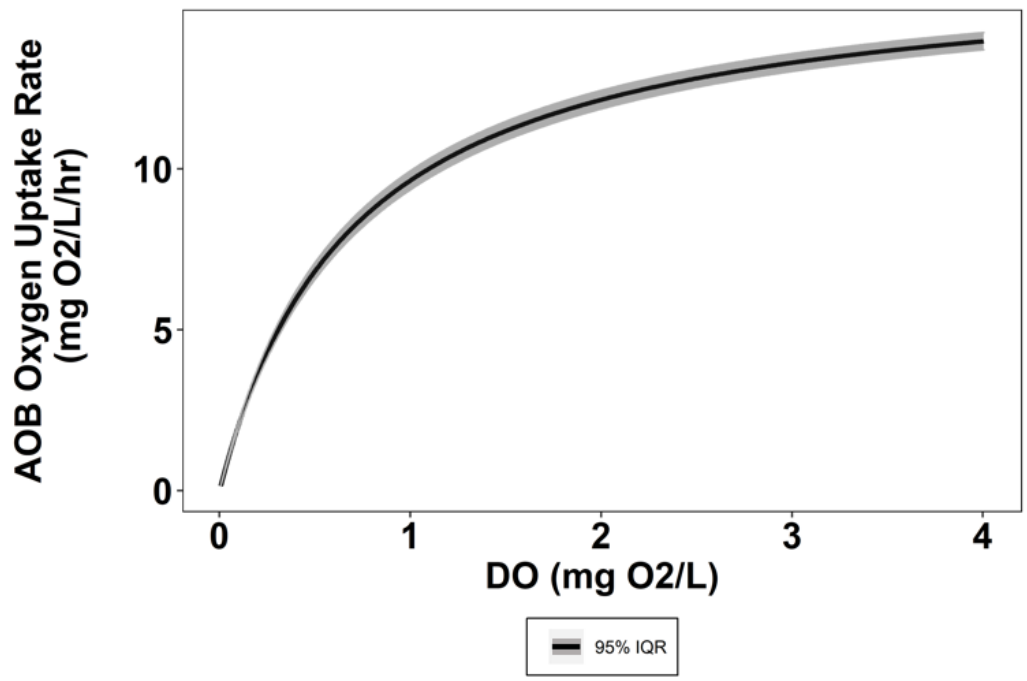

Figure 41. (6-2-2021 VIP Test #2) Final AOB OUR curve (with 95% IQR) from combined MCMC analysis.

Floc Photos

VIP Treatment Plant

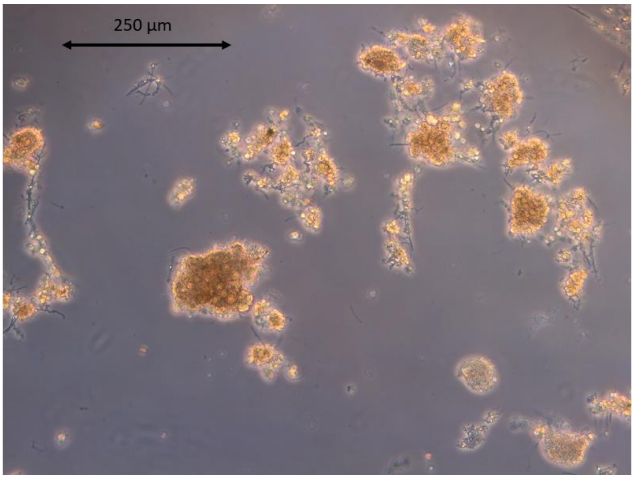

Figure 42. Floc photo #1 of VIP biomass sample.

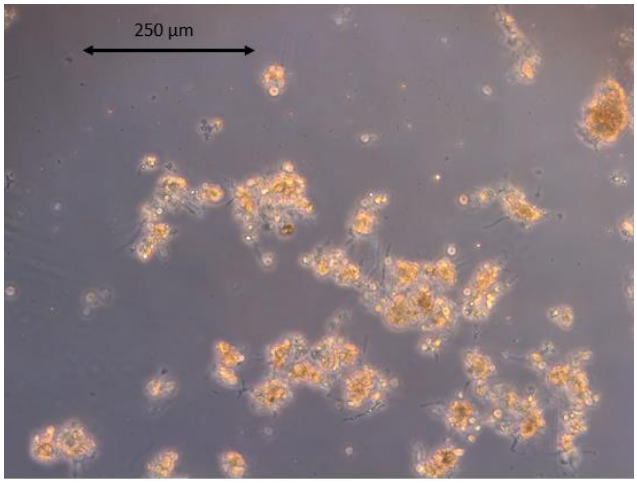

Figure 43. Floc photo #2 of VIP biomass sample.

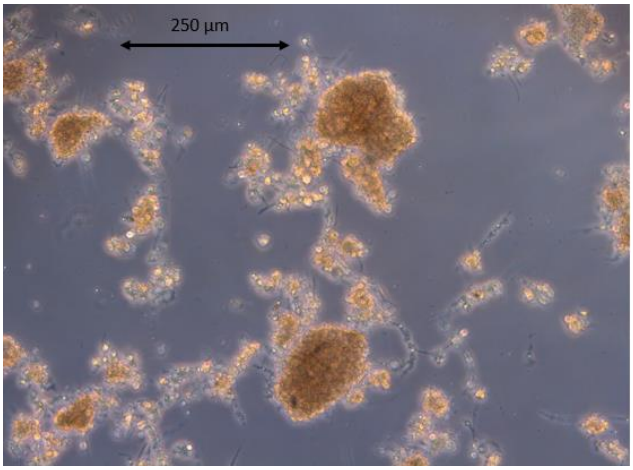

Figure 44. Floc photo #3 of VIP biomass sample.

Army Base Treatment Plant

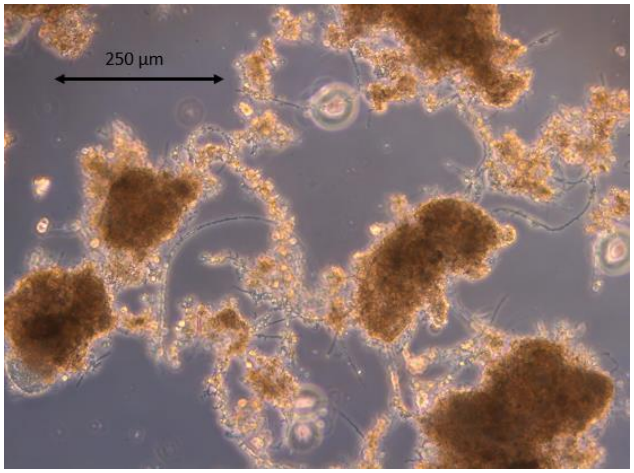

Figure 45. Floc photo #1 of ABTP biomass sample.

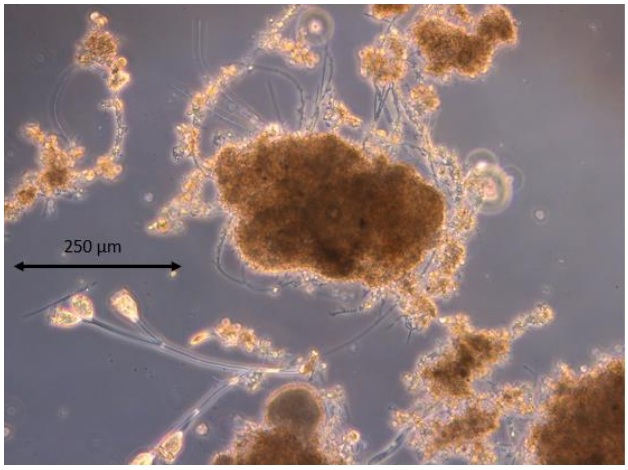

Figure 46. Floc photo #2 of ABTP biomass sample.

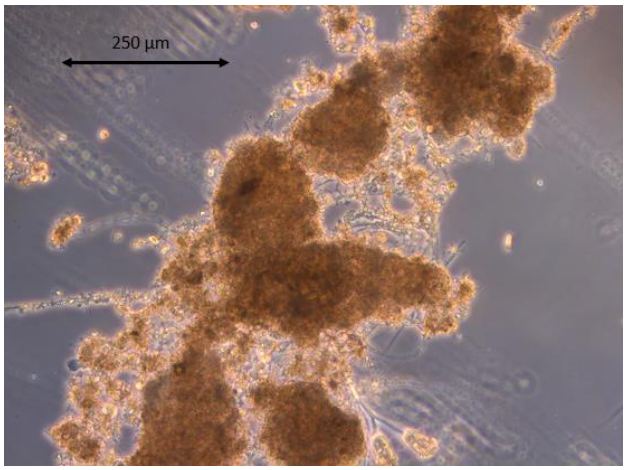

Figure 47. Floc photo #3 of ABTP biomass sample.

King William Treatment Plant

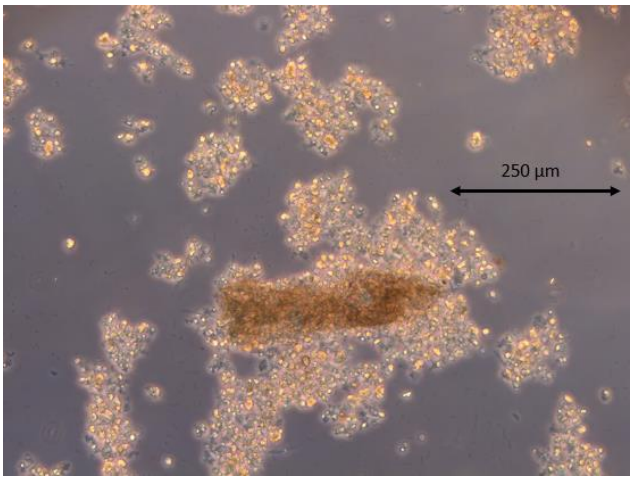

Figure 48. Floc photo #1 of KWTP biomass sample.

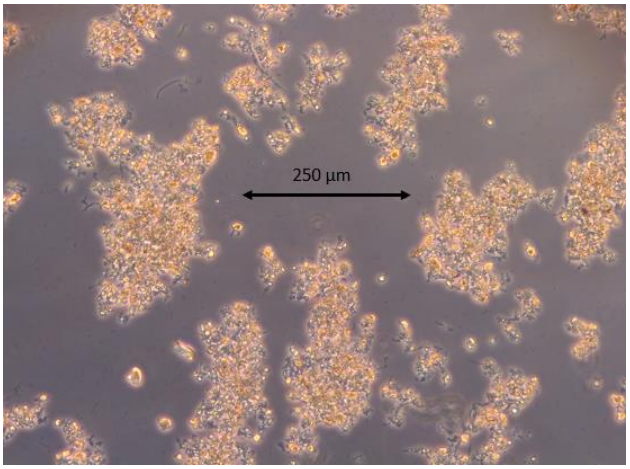

Figure 49. Floc photo #2 of KWTP biomass sample.

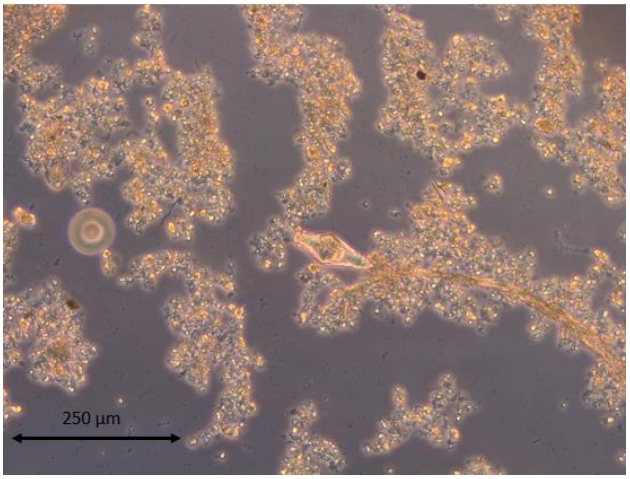

Figure 50. Floc photo #3 of KWTP biomass sample.

DO Probe Response Time Determination

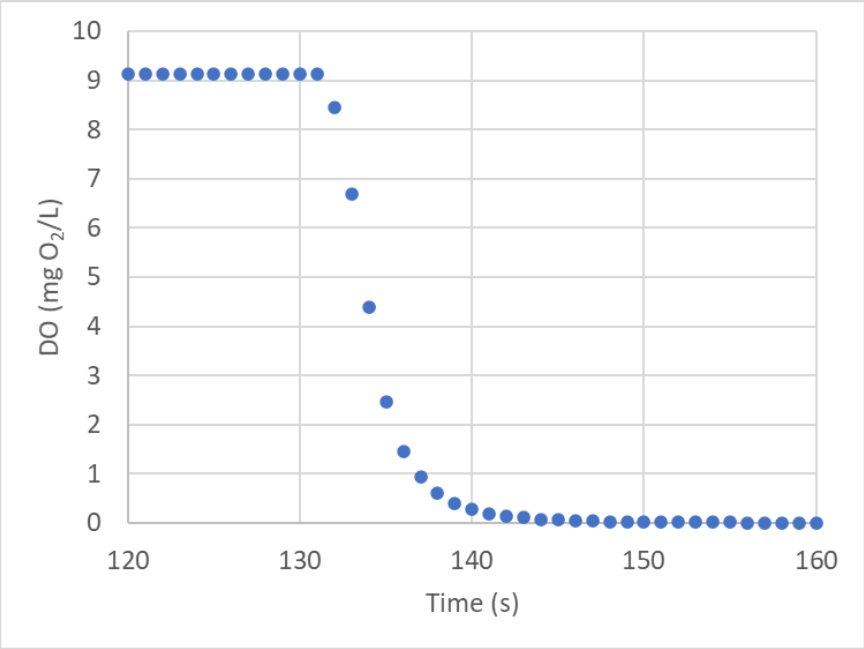

Figure 51. Experimental probe response time curve. Data points represent exposing probe to DO saturated water followed by quickly switching to zero DO water (using sodium sulfite).